TenSyGrid

Tensors for System Analysis of
Converter-dominated Power Grids

D 3.2 Generation Multilinear Models and Validation

by eRoots

Public

Co-funded by
the European Union

Supported by:

Federal Ministry
for Economic Affairs
and Energy

on the basis of a decision
by the German Bundestag

MINISTERIO
DE CIENCIA, INNOVACIÓN
Y UNIVERSIDADES

AGENCIA
ESTATAL DE
INVESTIGACIÓN

CDTI
INNOVACIÓN

XJENZA
MALTA

This research was funded by CETPartnership, the Clean Energy Transition Partnership under the 2023 joint call for research proposals, co funded by the European Commission (GA 101 069750) and with the funding organizations detailed on https://cetpartnership.eu/funding-agencies-and-call-modules.

About TenSyGrid

The demand for the power grid in Europe is undergoing profound changes due to an increasing number of decentralized feed-in points and the fluctuating supply from renewable energies. This complexity in interactions between power grid components poses a challenge for maintaining system stability. To address this, the European project TenSyGrid is developing a toolbox for direct stability assessment using multilinear models to capture the complex dynamics of power grid components. The objective is to support grid operators in assessing large power grids primarily powered by renewable energy. The toolbox will be compatible with existing commercial software packages to facilitate integration into current workflows.

Project Title	Tensors for System Analysis of Converter-dominated Power Grids
Programme	Horizon Europe - Clean Energy Transition Partnership (CETP)
Project Number	CETP-FP-2023-00138
Project Type	Research-oriented approach (ROA)
Call Module	CM2023-02 Energy system flexibility: renewables production, storage and system integration
Transition Initiative	TRI1 Net-zero emissions energy system
Project Start	01.12.2024
Project Duration	3 years
Coordinator	Fraunhofer IWES
Project Website	`www.tensygrid.eu`

Consortium

Fraunhofer IWES (Project Coordinator)

CITCEA UPC

eRoots

HAW HAMBURG

L-Università ta' Malta

About this document

Deliverable Number	D 3.2
Title	Generation Multilinear Models and Validation
Work Package	3
Leading Partner	eRoots Analytics
Authors	Pablo de Juan Vela Marina Rosés Gilbert Maria Sans Esqué Josep Fanals i Batllori Dr. Eduardo Prieto Araujo
Reviewers	Dr. Eduardo Prieto Araujo
Version	V1.0
Due Date	30.11.2025
Version Date	28.11.2025
Reviewer Accepted	28.11.2025
WP Leaders Accepted	28.11.2025

Dissemination Level	
PU	Public

Summary

This document focuses on the development of generation models for various components found in modern power systems. The devices studied include generators, their associated control systems such as exciters (for voltage control), governors (for frequency control), and stabilizers. The work also addresses other elements like power converters. The primary objective was to take the complex, real-world behavior of these devices, which are usually described by non-linear differential equations, and reformulate them into simpler multi-linear equations applying the work from work package 1. Significantly, the models include key non-linear effects like saturations, trigonometric transformations and other non multi linear functions. These functions were subjected to a reformulation process that gave rise to mathematically equivalent multi linear models. This multi-linear models maintain the original complexity while enabling the use of powerful tensor-based tools in the context of *TenSyGrid*. The ultimate objective of this multi-linearization is to express the resulting multi-linear equations in tensor form to speed up the computations.

After the multi-linear models were defined, we proceeded to validate their accuracy. We used the numerical simulation software, *VeraGrid* to run time simulations of the different models. The results from these simulations were then compared against the reference non-linear models. This comparison confirmed that the multi-linear reformulations were accurate and represented with fidelity the actual dynamic behavior of the different generation models when integrated into a complete electrical system. The simulations tested the models across multiple ranges of transients and steady-state conditions, verifying their reliability under diverse operating scenarios.

Contents

List of Figures

List of Tables

1 GENQEC Generator

The GenQEC (Generator with Quadratic-Exponential Characteristics) model represents a synchronous generator equipped with detailed excitation and control dynamics. It captures the non-linear magnetic behaviour of the generator, particularly through saturation functions applied to the main field and armature reaction.

The model was chosen to provide a high fidelity representation of the synchronous machine dynamics. It is mathematically defined in the d-q reference frame, utilizing rotor flux linkages (Ψ_d, Ψ_q) as state variables. The model explicitly captures a big range dynamic response, including both transient forces (E'_d, E'_q), while incorporating Quadratic-Exponential saturation functions. The model also includes a big array of non multilinear functions that can be challenging to model using tensors.

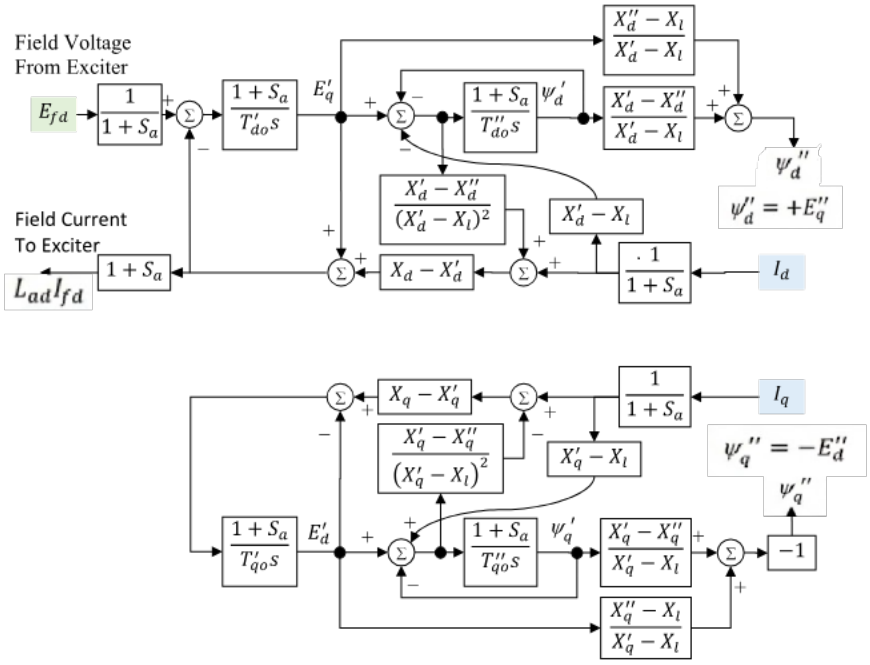

Figure 1.1: Block diagram of the GENQEC generator. [1]

1.1 Non-linear model

Parameters

Symbol	Description	Unit
ω_s	Synchronous speed	rad/s
R_s	Stator resistance	Ω
X_{dsat}	Saturated direct-axis synchronous reactance	Ω
X'_{dsat}	Saturated direct-axis transient reactance	Ω
X_{qsat}	Saturated quadrature-axis synchronous reactance	Ω
X'_{qsat}	Saturated quadrature-axis transient reactance	Ω
X''_{dsat}	Saturated direct-axis subtransient reactance	Ω
X''_{qsat}	Saturated quadrature-axis subtransient reactance	Ω
X_{ls}	Stator leakage reactance	Ω
T'_{d0sat}	Saturated direct-axis transient time constant	s
T''_{d0sat}	Saturated direct-axis subtransient time constant	s
T'_{q0sat}	Saturated quadrature-axis transient time constant	s
T''_{q0sat}	Saturated quadrature-axis subtransient time constant	s
H	Inertia constant	s

Variables

Symbol	Description	Unit
Ψ_d	d-axis flux linkage	Wb
Ψ_q	q-axis flux linkage	Wb
Ψ_0	Zero-sequence flux linkage	Wb
Ψ_{1d}	Flux linkage associated with X''_{dsat}	Wb
Ψ_{2q}	Flux linkage associated with X''_{qsat}	Wb
I_d	d-axis current	A
I_q	q-axis current	A
I_0	Zero-sequence current	A
V_d	d-axis voltage	V
V_q	q-axis voltage	V
V_0	Zero-sequence voltage	V
E_{fd}	Field voltage	V
E'_q	Transient voltage behind transient reactance in d-axis	V
E'_d	Transient voltage behind transient reactance in q-axis	V
δ	Rotor angle	rad
ω	Electrical rotational speed	rad/s
T_m	Mechanical torque	Nm
T_{fw}	Windage and friction torque	Nm
Sat_d	Saturation factor for the d-axis	–
Sat_q	Saturation factor for the q-axis	–

1.1.1 Electrical dynamics equations

$$
\begin{aligned}
V_d &= \frac{\omega}{\omega_s} E''_d + I_q X''_{q,sat} - I_d R_a \\
V_q &= \frac{\omega}{\omega_s} E''_q - I_d X''_{d,sat} - I_q R_a \\
\frac{1}{\omega_s}\frac{d\Psi_0}{dt} &= R_s I_0 + V_0 \\
E''_q &= E_{q1} + E_{q2} - I_d(X_{d,sat} - X''_{d,sat}) \\
E''_d &= E_{d1} + E_{d2} + I_q(X_{q,sat} - X''_{q,sat}) \\
E'_q &= E_{q1} + E_{q2} - \frac{X'_{d,sat} - X''_{d,sat}}{X_{d,sat} - X''_{d,sat}} E_{q2} - I_d(X_{d,sat} - X'_{d,sat}) \\
E'_d &= E_{d1} + E_{d2} - \frac{X'_{q,sat} - X''_{q,sat}}{X_{q,sat} - X''_{q,sat}} E_{d2} + I_q(X_{q,sat} - X'_{q,sat}) \\
T''_{d0,sat}\frac{dE''_q}{dt} &= -\frac{X'_{d,sat} - X''_{d,sat}}{X_{d,sat} - X''_{d,sat}} E_{q2} \\
T''_{q0,sat}\frac{dE''_d}{dt} &= -\frac{X'_{q,sat} - X''_{q,sat}}{X_{q,sat} - X''_{q,sat}} E_{d2} \\
T'_{d0,sat}\frac{dE'_q}{dt} &= E_{fd,sat} - E_{q1} \\
T'_{q0,sat}\frac{dE'_d}{dt} &= -E_{d1}
\end{aligned}
$$

1.1.2 Swing equations

$$
\frac{d\delta}{dt} = \omega - \omega_s \tag{1.1}
$$

$$
\frac{2H}{\omega_s}\frac{d\omega}{dt} = T_m - (\Psi_d I_q - \Psi_q I_d) - T_{fw} \tag{1.2}
$$

Electrical Torque Equations

$$
\Psi_q = \Psi''_q - I_q X''_{qsat} = -E''_d - I_q X''_{qsat} \tag{1.3}
$$

$$
\Psi_d = \Psi''_d - I_d X''_{dsat} = E''_q - I_d X''_{dsat} \tag{1.4}
$$

$$
T_{elec} = \Psi_d I_q - \Psi_q I_d \tag{1.5}
$$

Transient Internal Voltages

$$E_{q1} = E''_q + (E'_q - E''_q)\frac{X_{dsat} - X''_{dsat}}{X_{dsat} - X'_{dsat}} = \frac{X_{dsat} - X''_{dsat}}{X_{dsat} - X'_{dsat}}E'_q - \frac{X_{dsat} - X'_q}{X_{dsat} - X'_{dsat}}E''_q \tag{1.6}$$

$$E_{d1} = E''_d + (E'_d - E''_d)\frac{X_{qsat} - X''_{qsat}}{X_{qsat} - X'_{qsat}} = \frac{X_{qsat} - X''_{qsat}}{X_{qsat} - X'_{qsat}}E'_d - \frac{X_{qsat} - X'_d}{X_{qsat} - X'_{qsat}}E''_d \tag{1.7}$$

$$E_{q2} = -(E'_q - E''_q)\frac{X_{dsat} - X'_{dsat}}{X_{dsat} - X''_{dsat}} + I_d(X_{dsat} - X''_{dsat}) \tag{1.8}$$

$$E_{d2} = -(E'_d - E''_d)\frac{X_{qsat} - X'_{qsat}}{X_{qsat} - X''_{qsat}} - I_q(X_{qsat} - X''_{qsat}) \tag{1.9}$$

1.1.3 Saturations

$$X''_{dsat} = \frac{X''_d - X_l}{Sat_d} + X_l \tag{1.10}$$

$$X''_{qsat} = \frac{X''_q - X_l}{Sat_q} + X_l \tag{1.11}$$

$$X'_{dsat} = \frac{X'_d - X_l}{Sat_d} + X_l \tag{1.12}$$

$$X'_{qsat} = \frac{X'_q - X_l}{Sat_q} + X_l \tag{1.13}$$

$$X_{dsat} = \frac{X_d - X_l}{Sat_d} + X_l \tag{1.14}$$

$$X_{qsat} = \frac{X_q - X_l}{Sat_q} + X_l \tag{1.15}$$

$$T'_{d0sat} = \frac{T'_{d0}}{Sat_d} \tag{1.16}$$

$$T'_{q0sat} = \frac{T'_{q0}}{Sat_q} \tag{1.17}$$

$$T''_{d0sat} = \frac{T''_{d0}}{Sat_d} \tag{1.18}$$

$$T''_{q0sat} = \frac{T''_{q0}}{Sat_q} \tag{1.19}$$

$$E_{fdsat} = \frac{E_{fd}}{Sat_d} \tag{1.20}$$

$$X_{mdsat} I_{fd} = (X_{dsat} - X_l) I_{fd} = \frac{X_d - X_l}{Sat_d} I_{fd} \tag{1.21}$$

1.1.4 Changes in saturation calculation

The three following functions are the most commonly used to calculate the saturation:

- **Quadratic:**

  $$\text{Sat}(x) = B(x - A)^2$$

  Used in GE PSLF and PowerWorld Simulator [1].

- **Scaled Quadratic:**

  $$\text{Sat}(x) = \frac{B(x - A)^2}{x}$$

Used in PTI PSS/E and PowerWorld Simulator [1].

- **Exponential:**

$$\text{Sat}(x) = Bx^A$$

Used in BPA-IPF and some specific models of PTI PSS/E and PowerWorld Simulator.

It is important to note that these saturation functions are only active when $x \leq A$. This can be expressed as follows

$$\text{Sat}_{\text{actual}}(x) = \begin{cases} x, & \text{if } x \leq A \\ \text{Sat}(x), & \text{if } x > A \end{cases} \tag{1.22}$$

In the simulator we model this condition as:

$$\text{Sat}_{\text{actual}}(x) = \frac{1}{2}(\text{Sat}(x) + \sqrt{\text{Sat}(x)^2}) \tag{1.23}$$

- **Hard Saturation:**

$$\text{Sat}(x) = A(x - B)\,\mathbf{1}_{\{x>B\}}$$

We also add a Hard Saturation to test the multilinear reformulation of non continuous equations.

In this case, the variable will be the magnetic flux

$$S_a = \text{Sat}(\Psi_{ag})$$

which is calculated using the air gap voltage as follows:

$$\Psi_{ag} = \frac{\omega_s}{\omega}\sqrt{V_{q,ag}^2 + V_{d,ag}^2}$$

where

$$V_{q,ag} = V_q + I_q R_a + I_d X_l \quad \text{and} \quad V_{d,ag} = V_d + I_d R_a - I_q X_l$$

Then, the saturation of each axis is calculated as:

$$\text{Sat}_d = \text{Sat}_q = 1 + S_a$$

1.2 Grid Interface Equations

The generator is connected to the grid through the following equations:

$$V_d - (-V_g \sin(\delta_g - \delta)) = 0, \tag{1.24}$$
$$V_q - (V_g \cos(\delta_g - \delta)) = 0, \tag{1.25}$$
$$P_g - (V_d I_d + V_q I_q) = 0, \tag{1.26}$$
$$Q_g - (V_q I_d - V_d I_q) = 0. \tag{1.27}$$

where V_g, δ_g, P_g, Q_g are the voltage magnitude, voltage angle, active power and reactive power at the bus where the generator is connected. This equations are the power balance equations at the bus expressed in the dq reference frame of the generator.

1.3 Multilinear model

The main non multilinearities in the model arise from division that can be easily multilinearized by multiplying accordingly and by the saturation. We focus on finding multilinear equations for these second variables. In the following section we use the work of [2] to multilinearize the different saturation functions that are defined by rational or exponential functions.

For this we take the equation:

$$\Psi_{ag} = \frac{\omega_s}{\omega}\sqrt{V_{q,ag}^2 + V_{d,ag}^2}$$

which then becomes the following by adding the auxiliary variables $u^{V_d}, u^{V_q}, u^{\omega}, u^{\Psi_{ag}}$:

$$u^{V_d} = V_{d,ag} \tag{1.28}$$
$$u^{V_q} = V_{q,ag} \tag{1.29}$$
$$u^{\omega} = \omega \tag{1.30}$$
$$u^{\Psi_{ag}} = \Psi_{ag} \tag{1.31}$$
$$\Psi_{ag} u^{\Psi_{ag}} (1+\omega)(1+u^{\omega}) = u^{V_d} V_{d,ag} + u^{V_q} V_{q,ag} \tag{1.32}$$

Now we take the equation:

$$S_a = \text{Sat}(\Psi_{ag})$$

The type of saturation changes the multilinear expression, beginning with the quadratic we get that:

$$S_a = B(\Psi_{ag} - A)^2 \tag{1.33}$$

$$u^{\Psi_{ag}} = \Psi_{ag} \tag{1.34}$$
$$S_a = B(\Psi_{ag} - A)(u^{\Psi_{ag}} - A) \tag{1.35}$$

We do the same for the scaled quadratic saturation:

$$S_a = B\frac{(\Psi_{ag} - A)^2}{\Psi_{ag}}$$

$$u^{\Psi_{ag}} = \Psi_{ag} \tag{1.36}$$
$$\Psi_{ag} S_a = B(\Psi_{ag} - A)(u^{\Psi_{ag}} - A) \tag{1.37}$$

And for the exponential saturation, if we suppose $A = \frac{p}{q}$ with $p, q \in \mathcal{N}$ and add $\max(p, q)$ auxiliary variables we get that:

$$S_a = B(\Psi_{ag} - A)^A$$

$$v_i^{\Psi_{ag}} = \Psi_{ag} \quad \forall i \in \{1, \max(p, q)\} \tag{1.38}$$
$$u_q^{\Psi_{ag}} = \prod_{i=1}^{q}(v_i^{\Psi_{ag}} - A) \tag{1.39}$$
$$u_p^{\Psi_{ag}} = \prod_{i=1}^{p}(v_i^{\Psi_{ag}} - A) \tag{1.40}$$
$$u_q^{\Psi_{ag}} S_a = B u_p^{\Psi_{ag}} \tag{1.41}$$
$$\tag{1.42}$$

This reformulation can actually be simplified by using a smart reordering and using $\log_2(\max(p, q))$ new auxiliary variables instead of $\max(p, q)$ [2].

Additionally, we also need to make sure the saturation is only active when $A \geq 0$. In the non multi linear model we achieved this by adding the constraint $\text{Sat}_{\text{actual}}(x) = \frac{1}{2}(\text{Sat}(x) + \sqrt{\text{Sat}(x)^2})$ we add the following auxiliary variables to multilinear the expression. Where 1.47 and 1.48 ensure u_1 and v_1 are positive and 1.46 ensures $u_1 = |x|$.

$$\mathrm{Sat}_{\text{actual}}(x) := \mathrm{Sat}_{\text{actual}}(x)\mathbf{1}_{x \geq A} \tag{1.43}$$

$$\mathrm{Sat}_{\text{actual}}(x) = \frac{1}{2}(x + v_1) \tag{1.44}$$

$$u_1 u_2 = x x_{aux} \tag{1.45}$$

$$v_1 v_2 = u_1 \tag{1.46}$$

$$w_1 w_2 = v_1 \tag{1.47}$$

$$x = x_{aux} \tag{1.48}$$

$$u_1 = u_2 \tag{1.49}$$

$$v_1 = v_2 \tag{1.50}$$

$$w_1 = w_2 \tag{1.51}$$

For the hard saturation we use the positive part decomposition to add the following equations:

$$(\Psi_{ag} - B) = u_1 u_2 - v_1 v_2 \tag{1.52}$$

$$u_1 u_2 v_1 v_2 = 0 \tag{1.53}$$

$$u_1 - u_2 = 0 \tag{1.54}$$

$$v_1 - v_2 = 0 \tag{1.55}$$

$$\tag{1.56}$$

where we have that

$$u_1 u_2 := \max(\Psi_{ag} - B, 0) \quad v_1 v_2 := -\min(\Psi_{ag} - B, 0) \tag{1.57}$$

In the end the saturation equation becomes:

$$S_a = A u_1 u_2 \tag{1.58}$$

Finally, we tackle the change of variable of the $\cos$ and $\sin$ functions that appear in the grid connection equations. We follow the work of [3] by adding the auxiliary variables $u^{\cos}, u^{\sin}$ and add the following equations. This reformulation is a simplified version of the one found in [3] where the normalizing term is avoided.

$$u^{\cos} := \cos(\delta_g - \delta) \tag{1.59}$$

$$u^{\sin} := \sin(\delta_g - \delta) \tag{1.60}$$

$$\frac{\partial u^{\cos}}{\partial t} = -u^{\sin}\left(\frac{\partial \delta_g}{\partial t} - \frac{\partial \delta}{\partial t}\right) \tag{1.61}$$

$$\frac{\partial u^{\sin}}{\partial t} = u^{\cos}\left(\frac{\partial \delta_g}{\partial t} - \frac{\partial \delta}{\partial t}\right) \tag{1.62}$$

1.4 Validation

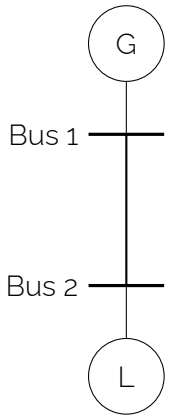

Figure 1.2: Validation Setup.

For the validation we study a grid consisting of two buses, one generator connected to the first bus, and a load connected to the other bus. Both buses are connected through a line. The system is represented in 1.2. The GENQEC generator is connected to the first bus with no other components (such as governor, exciter, etc) to simulate those we fix the values of the mechanical torque and the excitation field voltage to the specific amounts that make the setup behave in stationary regime. The GENQEC generator parameters used in the simulation are shown in Table 1.1 and the saturation chosen is the hard saturation.

The objective of the simulation is to compare both models' transient response when a disturbance in the grid happens. For this purpose we run a simulation using the software tool VeraGrid [4] and we add a sudden loss of load at a $t = 1s$ of 0.1 p.u. in the second bus. The simulation is initialized and then runs for 5 seconds. The chose the Midpoint Implicit Euler method to solve the differential equation with a time step of $1e^{-3}$.

We compare the results of the reference and multi linear models. We observe that the results are very similar, particularly the saturation, cosine and sine functions which are the most critical

Table 1.1: Generator and System Parameters

Parameter Description	Symbol	Value	Unit
General System			
Nominal Frequency	f_n	50	Hz
Inertia Constant	M	3.5	s
Stator Resistance	R_s	0.003	p.u.
Reactances			
Synchronous Reactance (d-axis)	X_d	1.8	p.u.
Synchronous Reactance (q-axis)	X_q	1.7	p.u.
Transient Reactance (d-axis)	X'_d	0.3	p.u.
Transient Reactance (q-axis)	X'_q	0.55	p.u.
Subtransient Reactance (d-axis)	X''_d	0.25	p.u.
Subtransient Reactance (q-axis)	X''_q	0.25	p.u.
Leakage Reactance	X_l	0.15	p.u.
Time Constants			
Transient Open-Circuit TC (d-axis)	T'_{d0}	8.0	s
Transient Open-Circuit TC (q-axis)	T'_{q0}	0.4	s
Subtransient Open-Circuit TC (d-axis)	T''_{d0}	0.03	s
Subtransient Open-Circuit TC (q-axis)	T''_{q0}	0.05	s
Saturation Parameters			
Saturation Threshhold	A	1.0	None
Saturation Scaling	B	5.0	None
Setup Constants			
Fixed Mechanical Torque	T_m	0.0961	p.u.
Fixed Excitation Voltage	T_m	5.96	p.u.

variables because of the reformulation. Other variables such as the frequency (omega) and the angle also coincide. Numerically, both simulations have a similar performance.

1.4.1 Quadratic Saturation

In this test we run an identical setup except for the type of saturation used in the generation. In this case, we chose the quadratic saturation. We also change the values of the mechanical torque and the field voltage to still start in steady state to $T_m = 0.0746 p.u., E_{fd} = 0.853 p.u.$

In this particular setup we observe that the generator starts with an active saturation $Sa > 0$

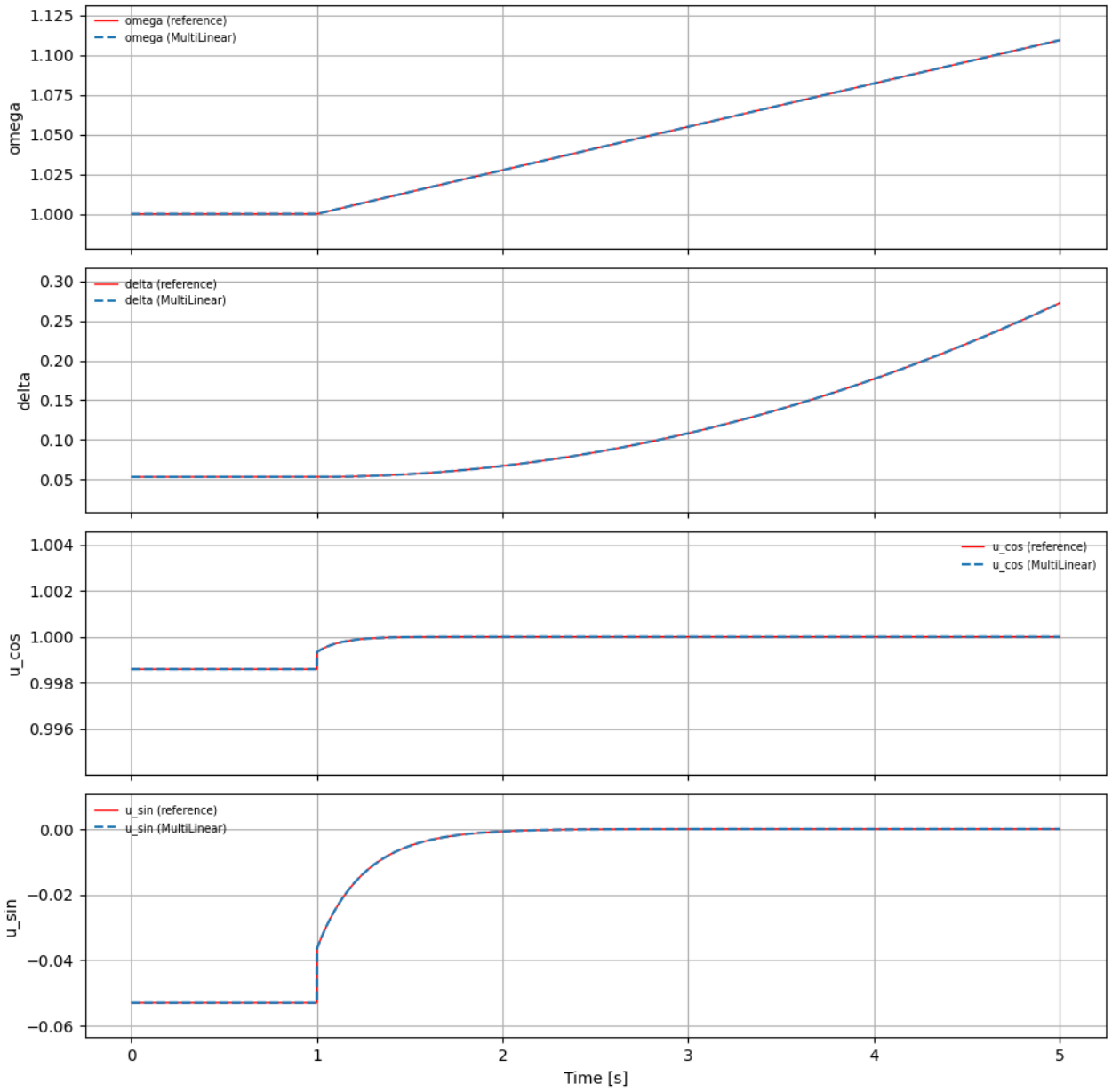

Figure 1.3: Simulation Results Comparison for the Hard Saturation Setup.

which then converges towards 0 after the loss of load. The multi linear and reference simulation are also extremely similar.

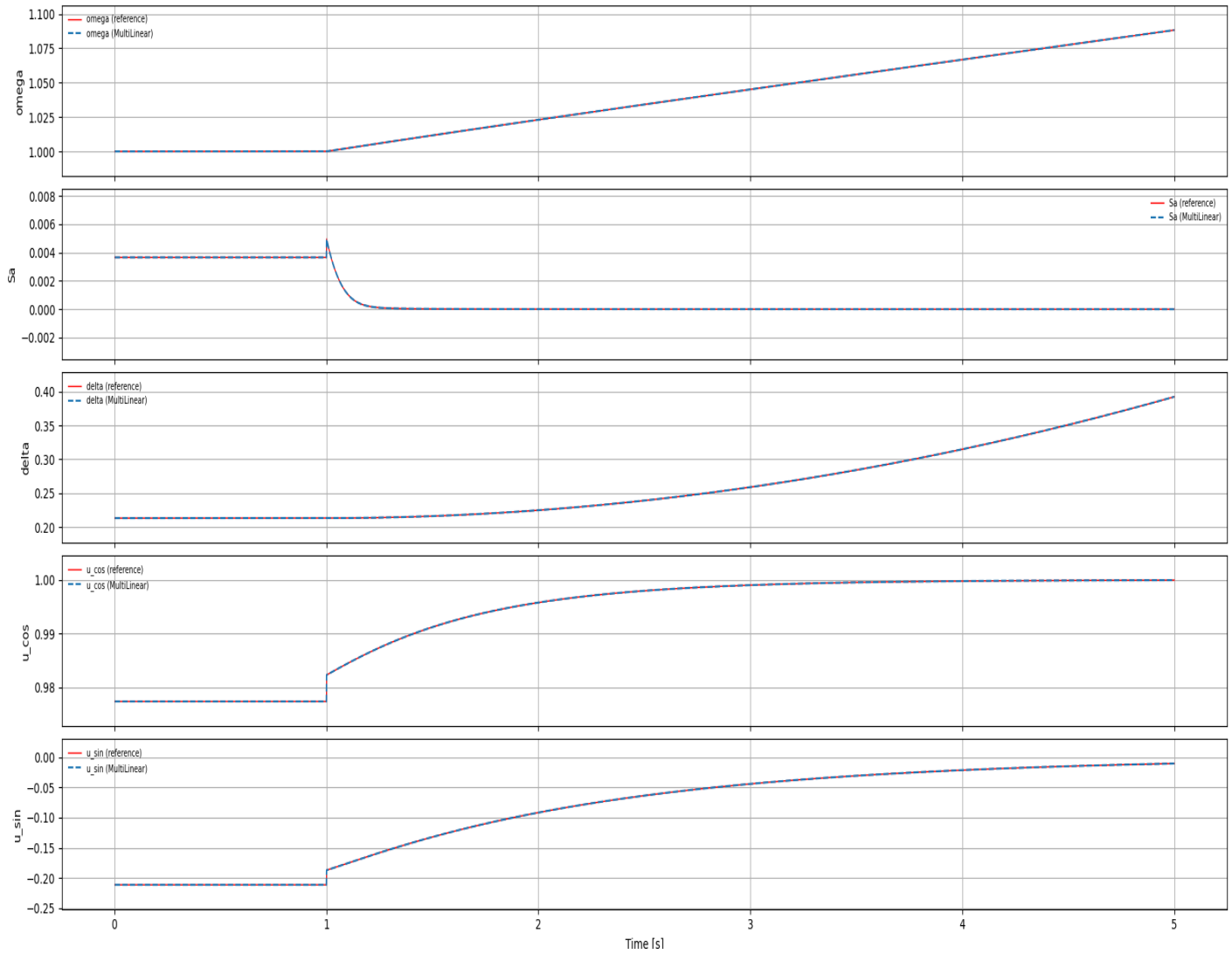

Figure 1.4: Simulation Results Comparison for the Quadratic Saturation.

2 IEEEG1 Governor

The IEEEG1 governor represents a classical steam turbine speed control system that adjusts the mechanical power T_m in response to frequency deviations in the generator. The governor therefore directly controls the active power balance of the entire unit, ensuring the generator remains synchronized with the grid.

The IEEEG1 governor is a speed control system for steam turbines that translates the speed error ($\Delta\omega$) through gain and lead-lag compensation to derive a desired steam flow. The model strictly incorporates physical constraints, including rate limits and position limits on the valve (represented by the hard saturations), before distributing the resulting steam flow across cascaded turbine stages to calculate the final mechanical power (P_m).

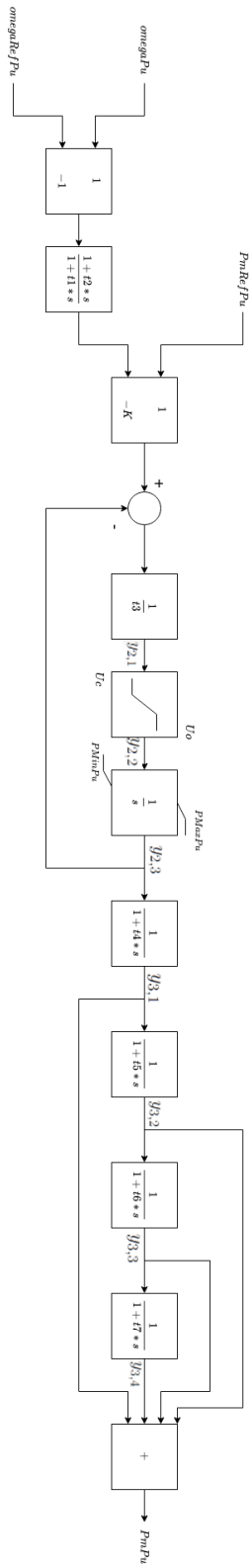

Figure 2.1: Block diagram of the IEEEG1 governor. [5]

2.1 Non-linear model

Variables

Symbol	Description	Unit
ω	Generator (rotor) speed	pu
P_e	Electrical power output	pu
P_{ref}	Reference (commanded) power	pu
P_{mwset}	Power setpoint	pu
f_b	Feedback signal	–
y_1	Power transducer output	pu
e	Control error	pu
e_{sat}	Saturated control error	pu
y_3	Integrator state of PI controller	pu
T_m	Mechanical power (turbine output)	pu
$y_{2,1}$	Valve rate command (after limiter)	pu/s
$y_{2,2}$	Valve position (integrated signal)	pu
$y_{2,3}$	Valve position (after mechanical limits)	pu
$y_{3,1}$	Reheater stage 1 output	pu
$y_{3,2}$	Reheater stage 2 output	pu
$y_{3,3}$	Reheater stage 3 output	pu
$y_{3,4}$	Reheater stage 4 output	pu
T_{aux}	Auxiliary torque/power correction	pu
e_t	Integral state of the auxiliary PI controller	pu·s
u_1	Speed deviation	pu
x_2	Intermediate control signal	pu

Table 2.1: Variables of Governor Model

Parameters

Table 2.2: Parameters of Governor Model

Symbol	Description	Unit
K_p	Proportional gain of load controller	–
K_i	Integral gain of load controller	s^{-1}
T_{pelec}	Electrical power transducer time constant	s
P_{ref0}	Base reference power offset	pu
ω_{ref}	Reference speed	pu
$e_{\min}$, $e_{\max}$	Error saturation limits	pu
$I_{\min}$, $I_{\max}$	Integrator saturation limits	pu
K	Governor gain (inverse droop)	–
$P_{\max}$, $P_{\min}$	Mechanical power limits	pu
U_c, U_o	Valve closing and opening rate limits	pu/s
T_1, T_2	Lead–lag time constants (governor input)	s
T_3	Valve actuator time constant	s
T_4, T_5, T_6, T_7	Time constants of reheater and cross–over stages	s
K_1, K_2, K_3, K_4	Steam fractions (stage gains)	–
$K_p^{(c)}$, $K_i^{(c)}$	PI gains of auxiliary controller	–, s^{-1}
P_0	Scaling coefficient for auxiliary control	–

Power Measurement Dynamics The transducer delay is represented as a first–order transfer function:

$$\frac{Y_1(s)}{P_e(s)} = \frac{1}{1 + sT_{\text{pelec}}} \tag{2.1}$$

which corresponds to the time–domain equation:

$$T_{\text{pelec}} \frac{dy_1}{dt} + y_1 = P_e \tag{2.2}$$

Error Calculation

$$e = (-\omega + \omega_{\text{ref}}) f_b + P_{\text{mwset}} - y_1 \tag{2.3}$$

After applying saturation limits:

$$e_{\text{sat}} = \text{Hardsat}(e, e_{\min}, e_{\max}) := \begin{cases} e_{\max}, & \text{if } e > e_{\max} \\ e, & \text{if } e_{\min} \leq e \leq e_{\max} \\ e_{\min}, & \text{if } e < e_{\min} \end{cases} \tag{2.4}$$

Integral and Proportional Action The integral term is defined as:

$$\frac{dy_3}{dt} = K_i e_{\text{sat}} \tag{2.5}$$

and the final reference power output is:

$$P_{\text{ref}} = P_{\text{refo}} + K_p e_{\text{sat}} + y_3 \tag{2.6}$$

or equivalently:

$$P_{\text{ref}} = P_{\text{refo}} + K_p e + y_3 \tag{2.7}$$

2.1.1 Governor Model

The governor model represents a reheat steam turbine governor with optional control loops for power–frequency regulation.

Speed Deviation and Lead–Lag Dynamics

$$u_1 = \omega - \omega_{\text{ref}} \tag{2.8}$$

$$\frac{Y_1(s)}{u_1(s)} = \frac{1 + sT_2}{1 + sT_1} \tag{2.9}$$

$$T_1 \frac{dy_1}{dt} + y_1 = T_2 \frac{du_1}{dt} + u_1 \tag{2.10}$$

Valve Control Loop

$$x_2 = P_{m,\text{ref}} - K y_1 - y_{2,3} \tag{2.11}$$

$$y_2 = \frac{x_2}{T_3} \tag{2.12}$$

$$y_{2,1} = \text{sat}(y_2, U_c, U_o) \tag{2.13}$$

Valve position integration:

$$\frac{dy_{2,2}}{dt} = y_{2,1} \tag{2.14}$$

and mechanical valve position (limited):

$$y_{2,3} = \text{Hardsat}(y_{2,2}, P_{\min}, P_{\max}) \tag{2.15}$$

Reheater and Cross-Over Stages Each reheater stage is represented as a first order lag:

$$T_4 \frac{dy_{3,1}}{dt} + y_{3,1} = y_{2,3} \tag{2.16}$$

$$T_5 \frac{dy_{3,2}}{dt} + y_{3,2} = y_{3,1} \tag{2.17}$$

$$T_6 \frac{dy_{3,3}}{dt} + y_{3,3} = y_{3,2} \tag{2.18}$$

$$T_7 \frac{dy_{3,4}}{dt} + y_{3,4} = y_{3,3} \tag{2.19}$$

Mechanical Power Output

$$T_m = K_1 y_{3,1} + K_2 y_{3,2} + K_3 y_{3,3} + K_4 y_{3,4} + T_{\text{aux}} \tag{2.20}$$

Additionnally, the parameters always K_1, K_2, K_3, K_4 satisfy:

$$K_1 + K_2 + K_3 + K_4 = 1 \tag{2.21}$$

2.2 Grid Connection

The governor model takes it's input from the generator through the speed deviation ω and outputs the mechanical power T_m to the generator model.

2.3 Multilinear model

The only non multilinearity in the model arises from the saturation blocks. We focus on finding multilinear equations for these blocks. Applying [2] we can express the saturation as:

$$\text{HardSat}(x, x_{min}, x_{max}) = x_{min} + (x - x_{min})\mathbf{1}_{\{x>x_{min}\}} - (x - x_{max})\mathbf{1}_{\{x>x_{max}\}} \tag{2.22}$$
$$= x_{min} + (x - x_{min})^{+} - (x - x_{max})^{+} \tag{2.23}$$

Therefore we add to the model the following equations and auxiliary variables for each saturation block:

$$(x - x_{min}) = u_1 u_2 - v_1 v_2 \tag{2.24}$$
$$u_1 u_2 v_1 v_2 = 0 \tag{2.25}$$
$$u_1 - u_2 = 0 \tag{2.26}$$
$$v_1 - v_2 = 0 \tag{2.27}$$
$$\tag{2.28}$$

$$(x - x_{max}) = u_3 u_4 - v_3 v_4 \tag{2.29}$$
$$u_3 u_4 v_3 v_4 = 0 \tag{2.30}$$
$$u_3 - u_4 = 0 \tag{2.31}$$
$$v_3 - v_4 = 0 \tag{2.32}$$
$$\tag{2.33}$$

$$\text{HardSat}(x, x_{min}, x_{max}) = x_{min} + u_1 u_2 - u_3 u_4 \tag{2.34}$$

This way we replace the saturations on e, $y_{2,2}$ and $y_{2,3}$ by multi linear equations.

2.4 Validation

To extend the validation, we repeat the previous test but now including the governor model. The generator is equipped with the IEEEG1 defined previously, the remainder of the setup remains unchanged. The mechanical torque is no longer fixed, as the governor reacts dynamically to the active-power disturbance introduced at t=1 s. The trajectories of frequency, mechanical power, and rotor angle are again extremely similar, confirming that the governor dynamics are reproduced accurately.

Table 2.3: Governor-Turbine Model Parameters.

Symbol	Value	Description
		Governor Gain and Limits
$1/R$	10.0	**Governor Gain** (Inverse Droop).
$P_{\max}$	2.0	Maximum Mechanical Power output limit (pu).
$P_{\min}$	0.0	Minimum Mechanical Power output limit (pu).
U_c	-0.1	Maximum valve closing rate limit (pu/s).
U_o	0.1	Maximum valve opening rate limit (pu/s).
		Time Constants (All in seconds)
T_1	1.0	Governor actuator response time.
T_2	1.0	Steam Chest/Reheater time constant.
T_3	10.0	Crossover/Reset time constant for the loop.
T_4	0.2	High Pressure (HP) Turbine stage delay.
T_5	0.5	Intermediate Pressure (IP) Turbine stage delay.
T_6	0.1	Low Pressure (LP) Turbine stage delay 1.
T_7	0.05	Low Pressure (LP) Turbine stage delay 2.
		Steam Fractions (Distribution Factors)
K_1	0.5	Fraction of power from the HP stage (T_4).
K_2	0.5	Fraction of power from the IP stage (T_5).
K_3	0.0	Fraction set to zero (not used in this configuration).
		Reference Inputs
ω_{ref}	1.0	Reference speed (nominal synchronous speed).
P_{ref}	0.096	Initial steady-state mechanical power setpoint.

In the simulation, we observe that the governor adapts the mechanical torque delivered by the generator. We can see the hard saturation working properly when $y_{2,3gov}$ is equal to zero since the governor can not deliver less than 0 torque.

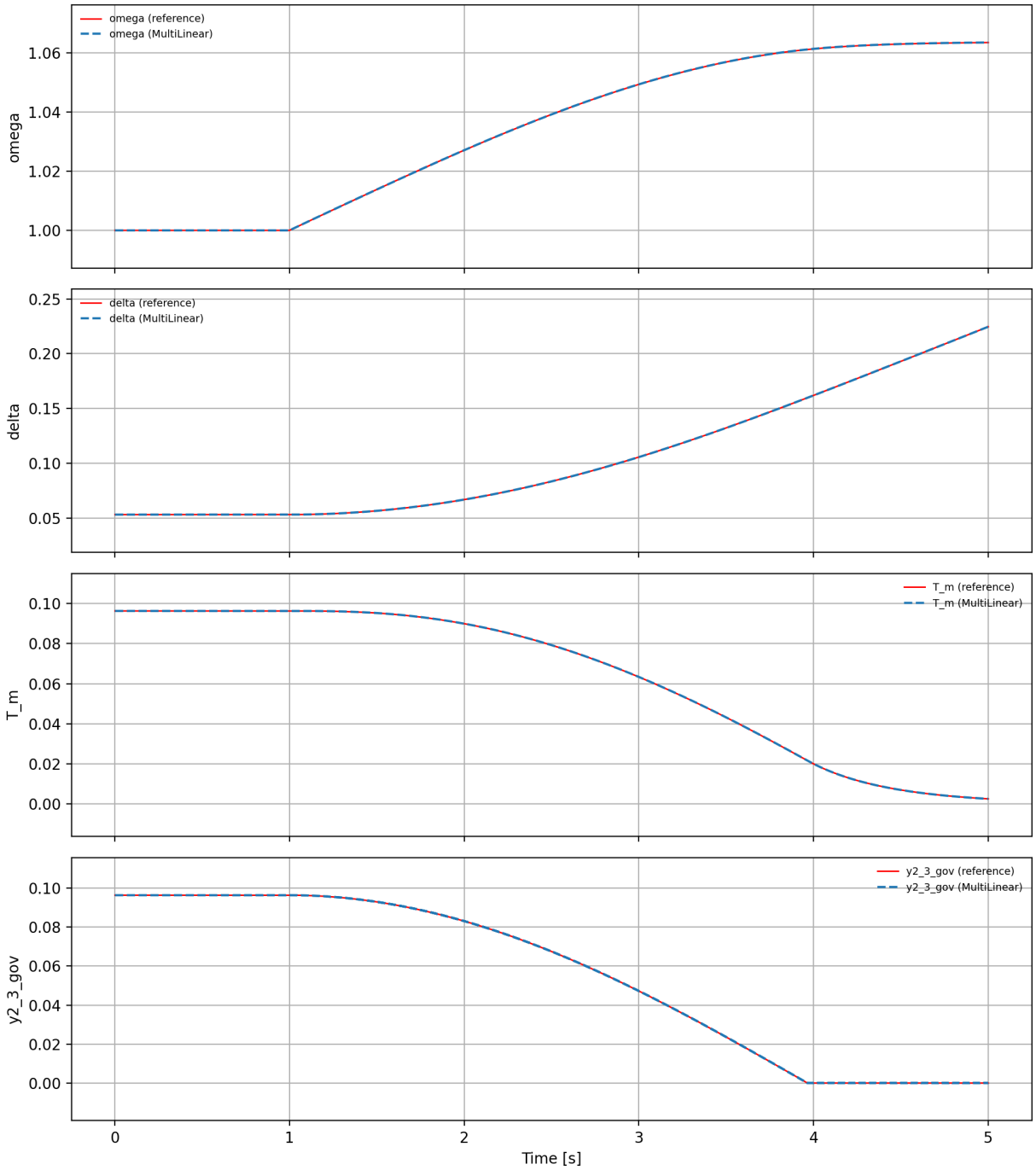

Figure 2.2: Simulation Results Comparison for the governor validation.

3 AC1C Exciter

The exciter provides the direct current field current to the rotor of a synchronous generator. By regulating this field current, it controls the generator terminal voltage and reactive power output, maintaining the desired voltage level under varying load and network conditions.

For this study, we selected the **IEEE Type AC1C** model, which represents an excitation system (rotating exciter) using non-controlled rectifiers. This model was chosen because it is a widely accepted industry standard that accurately captures the dynamics of field-controlled alternators, including magnetic saturation, and realistically represents the excitation systems commonly found in thermal power plants.

3.1 Non-linear model

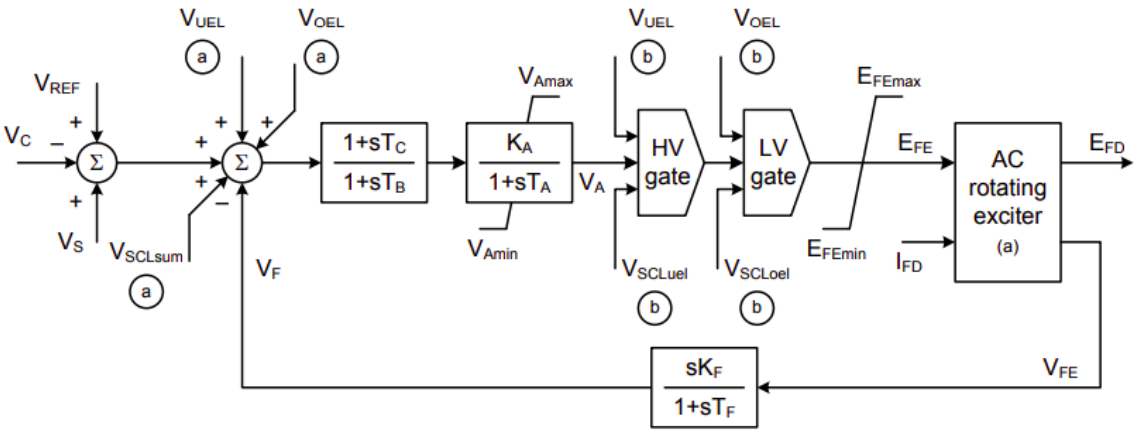

Figure 3.1: Block diagram of the AC1C exciter. [6]

Variables

Symbol	Description	Unit
I_R	Rotor current	pu
V_g	Stator voltage	pu
E_{fd}	Field voltage	pu
V_{pss}	Power system stabiliser output	pu
$U_{s,\text{ref}}$	Reference voltage	pu
V_e	Internal exciter voltage	pu
V_{fe}	Exciter field current signal	pu
E_{fe}	Exciter field voltage	pu
u_{aux}	Auxiliary algebraic variable	pu
$V_{e,\text{max}}^{pu}$	Exciter field voltage limit variable	pu
U_{SCL}	Stator current limiter signal	pu
U_{OEL}	Over-excitation limiter signal	pu
U_{UEL}	Under-excitation limiter signal	pu
U_{SCLUEL}	Combined stator/under-excitation limiter signal	pu
P_{SCL}	Stator current limiter selector position	–
P_{OEL}	Over-excitation limiter selector position	–
P_{UEL}	Under-excitation limiter selector position	–

Parameters

Symbol	Description	Unit
K_a	AVR gain	–
K_f	Exciter rate feedback gain	–
K_c	Rectifier loading factor	–
K_d	Demagnetising factor	–
K_e	Exciter field resistance constan0	–
t_A	AVR time constant2	s
t_B	Lag time constant	s
t_C	Lead time constant	s
t_E	Exciter field time constant	s
t_F	Rate feedback time constant	s
t_R	Stator voltage filter time constant	s
A_E	Saturation gain (0.02)	–
B_E	Saturation exponential coefficient	–
$V_{a,\max}^{pu}$	AVR output upper limit	pu
$V_{a,\min}^{pu}$	AVR output lower limit	pu
$E_{fe,\max}^{pu}$	Exciter field voltage upper limit	pu
$E_{fe,\min}^{pu}$	Exciter field voltage lower limit	pu
$V_{e,\min}^{pu}$	Exciter output lower limit	pu
$V_{fe,\max}^{pu}$	Exciter field current upper limit	pu
T_{ol}	Limit tolerance	–

3.1.1 Equations

$$\text{Voltage filter:} \quad \frac{dy_1}{dt} = \frac{1}{t_R}\left(V_g - y_1\right) \tag{3.1}$$

$$\text{Rate feedback:} \quad \frac{dy_2}{dt} = \frac{1}{t_F}\left(K_f E_{fd} - y_2\right) \tag{3.2}$$

$$\text{Lead–lag compensator:} \quad t_B\,\dot{y}_3 + y_3 = t_C\,\dot{e} + e, \qquad e = -y_1 + U_{s,\mathrm{ref}} + V_{\mathrm{pss}} - y_2 \tag{3.3}$$

$$\text{Amplifier:} \quad t_A\,\dot{y}_4 + y_4 = K_a\,y_3 \tag{3.4}$$

$$\text{Limiter:} \quad y_5 = \mathrm{Sat}(y_4, V_{a,\min}^{pu}, V_{a,\max}^{pu}) \tag{3.5}$$

Selector logic The exciter voltage E_{fe} is computed through the following equations depending on the status of the limiter signals and selector positions, for the stator current limiter (SCL), over-excitation limiter (OEL) and under-excitation limiter (UEL). This selectors are optional.

$$y_{5,1} = \min(U_{\text{SCL}}, y_5)\, P_{\text{SCL}}(P_{\text{SCL}} - 1) + y_5(P_{\text{SCL}} - 2) \tag{3.6}$$
$$y_{5,2} = \min(U_{\text{OEL}}, y_{5,1})\, P_{\text{OEL}}(P_{\text{OEL}} - 1) + y_{5,1}(P_{\text{OEL}} - 2) \tag{3.7}$$
$$y_{5,3} = \max(U_{\text{UEL}}, y_{5,2})\, P_{\text{UEL}}(P_{\text{UEL}} - 1) + y_{5,2}(P_{\text{UEL}} - 2) \tag{3.8}$$
$$y_{5,4} = \max(U_{\text{SCLUEL}}, y_{5,3})\, P_{\text{SCL}}(P_{\text{SCL}} - 1) + y_{5,3}(P_{\text{SCL}} - 2) \tag{3.9}$$
$$y_6 = \text{Sat}(y_{5,4}, E^{pu}_{fe,\min}, E^{pu}_{fe,\max}) \tag{3.10}$$
$$E_{fe} = y_6 \tag{3.11}$$

Sub-exciter model

$$x_1 = V^{pu}_{fe,\max} - K_d I_R \tag{3.12}$$
$$\text{error}_1 = E_{fe} - (K_d I_R + u_{\text{aux}}) \tag{3.13}$$
$$t_E \frac{dV_e^{\text{pre}}}{dt} = \text{error}_1 \tag{3.14}$$
$$V_e = \text{Hardsat}(V_e^{\text{pre}}, V^{pu}_{e,\min}, V^{pu}_{e,\max}) \tag{3.15}$$
$$u_{\text{aux}} = V_e K_e + V_e A E_x e^{-B E_x V_e} \tag{3.16}$$
$$V^{pu}_{e,\max} = \frac{V_{FEmax} - K_D I_R}{K_e + A E_x e^{-B E_x V_e}} \tag{3.17}$$
$$f_{\text{input}} = \frac{K_c I_R}{V_e} \tag{3.18}$$
$$f_{\text{output}} = F_{\text{rectifier}}\,(f_{\text{input}}) \tag{3.19}$$
$$E_{fd} = f_{\text{output}}\, V_e \tag{3.20}$$

The rectifier function can take multiple forms, here we define as defined in the IEEE standard

recommendation [6]:

$$f_{\text{exc}}(I_{\text{n}}) = \begin{cases} 0.577\, I_{\text{n}}, & \text{if } I_{\text{n}} < 0 \\ (1 - 0.577\, I_{\text{n}}), & \text{else if } 0 \leq I_{\text{n}} < 0.433 \\ \sqrt{0.75 - I_{\text{n}}^2}, & \text{else if } 0.433 \leq I_{\text{n}} < 0.75 \\ 1.732 - 1.732\, I_{\text{n}}, & \text{else if } 0.75 \leq I_{\text{n}} \leq 1.0 \\ 0, & \text{else } I_{\text{n}} > 1.0 \end{cases} \tag{3.21}$$

3.2 Grid Connection

The exciter takes multiples inputs from the generator and other components:

- V_g the bus voltage magnitude in p.u.
- V_{pss} the stabilizer output in p.u.
- I_r the rotor current in p.u. that is expressed as $E_{q1}Sat_q$ in the generator model.
- $U_{OEL}, U_{UEl}, U_{SCL}$ the limiter signals in p.u. that are computed in the over/under excitation limiters.

And then outputs the field voltage E_{fd} to the generator model.

3.3 Multilinear model

We change the hard saturations and the non linear rectifier function to multilinear equations. For the hard saturation we again use the apply the positive part decomposition and [2].

$$(y_4 - V_{a,\min}^{pu}) = u_1 u_2 - v_1 v_2 \tag{3.22}$$
$$u_1 u_2 v_1 v_2 = 0 \tag{3.23}$$
$$u_1 - u_2 = 0 \tag{3.24}$$
$$v_1 - v_2 = 0 \tag{3.25}$$
$$\tag{3.26}$$

$$(y_4, V^{pu}_{a,\min}) = u_3 u_4 - v_3 v_4 \tag{3.27}$$
$$u_3 u_4 v_3 v_4 = 0 \tag{3.28}$$
$$u_3 - u_4 = 0 \tag{3.29}$$
$$v_3 - v_4 = 0 \tag{3.30}$$
$$\tag{3.31}$$

$$HardSat(y_4, V^{pu}_{a,\min}, V^{pu}_{a,\max}) := V^{pu}_{a,\min} + u_1 u_2 - + u_3 u_4 \tag{3.32}$$

For the rectifier function we first use the Heaviside $H(x)$ function to rewrite it as:

$$\begin{aligned} f_{\text{exc}}(I_{\text{n}}) \; &= 0.577\, I_{\text{n}}\, H(-I_{\text{n}}) + \left[(1 - 0.577\, I_{\text{n}}) - \sqrt{0.75 - I_{\text{n}}^2}\right] H(0.433 - I_{\text{n}}) \\ &+ \left[\sqrt{0.75 - I_{\text{n}}^2} - (1.732 - 1.732\, I_{\text{n}})\right] H(0.75 - I_{\text{n}}) \\ &+ (1.732 - 1.732\, I_{\text{n}})\, H(1.0 - I_{\text{n}}) \end{aligned} \tag{3.33}$$

Then we use the positive part decomposition to rewrite each Heaviside function and add the corresponding multilinear equations. We first rewrite $H(-I_n)$ as:

$$-I_n = u_1 u_2 - v_1 v_2 \tag{3.34}$$
$$u_1 u_2 v_1 v_2 = 0 \tag{3.35}$$
$$u_1 - u_2 = 0 \tag{3.36}$$
$$v_1 - v_2 = 0 \tag{3.37}$$
$$\tag{3.38}$$

$$H_{I_n} := H(-I_n) \tag{3.39}$$
$$-I_n = u_1 u_2 \times H_{I_n} - v_1 v_2 (1 - H_{I_n}) \tag{3.40}$$
$$\tag{3.41}$$

We then repeat the same process for each Heaviside function in the rectifier equation. Additionally, we need to consider that multiple heaviside functions are present at the same time, so we need to compensate for that by adding the cancelling terms of the overlapping regions. This is helped by the fact that each heaviside function is greater or equal than the previous one.

3.4 Validation

We run the same experiment but enabling the exciter. In this case, the field voltage is controlled dynamically by the excitation system rather than being kept constant. The load perturbation at t=1 s triggers the expected voltage-regulation response. The time series shows a very similar output, which validates the implementation of the exciter in the multi-linear framework.

Table 3.1: Exciter Model Parameters (IEEE AC1C Structure)

Symbol	Value	Description
		Automatic Voltage Regulator (AVR) Parameters
K_a	50.0	AVR proportional gain.
T_a	0.2	AVR time constant (s).
$V_{a,\max}$	20.0	AVR output maximum limit (pu).
$V_{a,\min}$	-10.0	AVR output minimum limit (pu).
T_b	10.0	Lead-lag: Lag time constant (s).
T_c	1.0	Lead-lag: Lead time constant (s).
T_R	0.02	Stator voltage filter time constant (s).
		Exciter Field and Saturation Parameters
K_E	1.0	Exciter field resistance constant.
A_{Ex}	0.02	Gain of exciter saturation function (Submodel).
B_{Ex}	0.1	Exponential coefficient of exciter saturation (Submodel).
$E_{fe,\max}$	50.0	Max exciter field voltage (AVR input limit) (pu).
$E_{fe,\min}$	0.0	Min exciter field voltage (AVR input limit) (pu).
		Rectifier and Stabilization Parameters
K_f	0.03	Exciter rate feedback gain.
T_F	1.0	Exciter rate feedback time constant (s).
K_c	0.2	Rectifier loading factor.
K_d	0.1	Demagnetizing factor.

More specifically, 3.2 shows the output of the fied voltage E_{fd} and the exciter output voltage E_{fe}. We observe that the results of these internal variables coincide for the multi linear and the reference model.

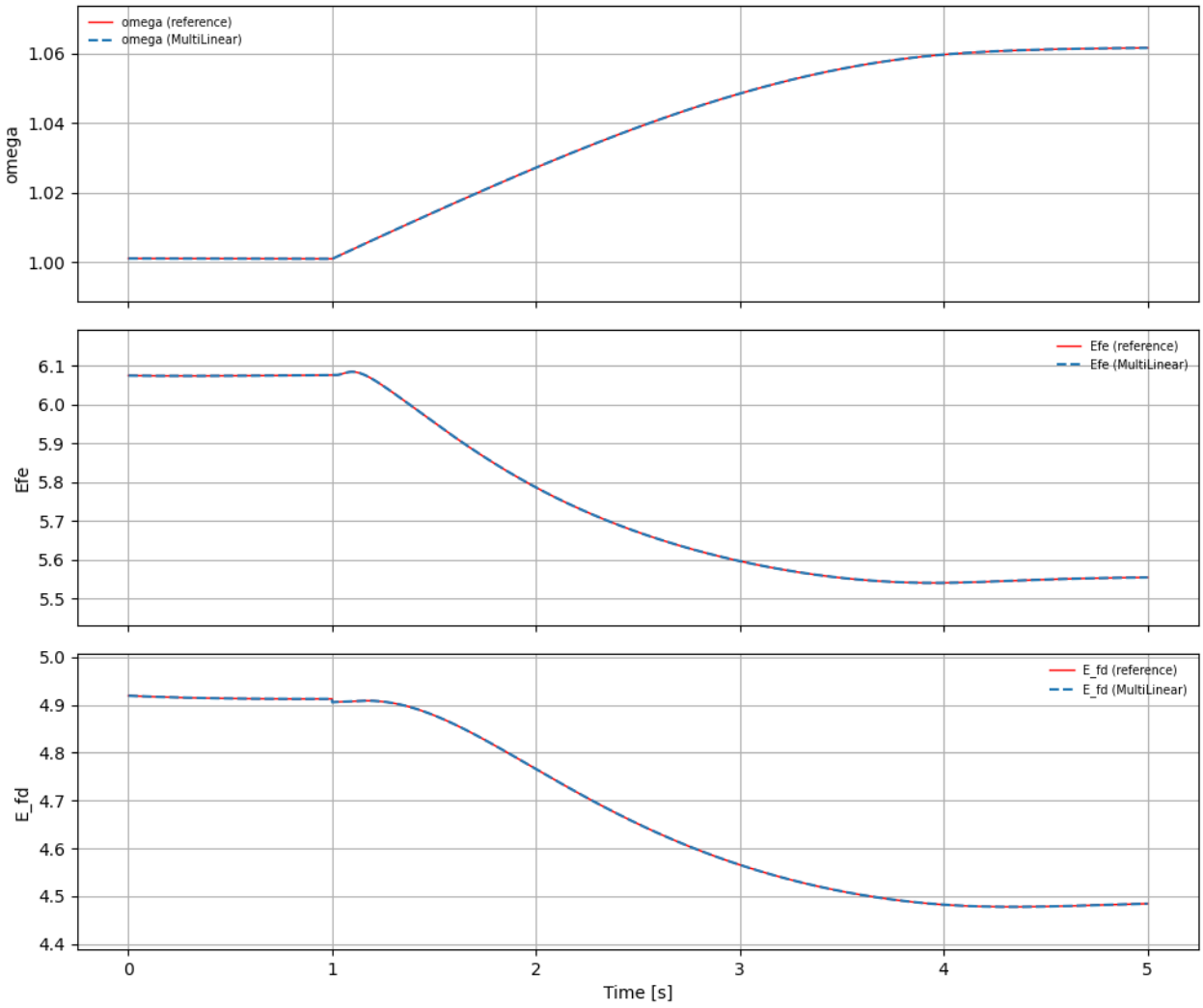

Figure 3.2: Exciter internal variables in simulation results.

4 PSS1A Stabilizer

The power system stabilizer (PSS) improves the dynamic stability of a synchronous generator by providing a supplementary control signal to the exciter. It introduces a damping torque that counteracts power oscillations following disturbances, helping to maintain steady operation of the power system.

The power system stabilizer works by sensing an input signal related to the generator's speed or accelerating power, which indicates the onset of oscillations. This signal is first processed through different filters and then processed in order to compensate the possible voltage oscillations. The output signal is then relayed to the exciter.

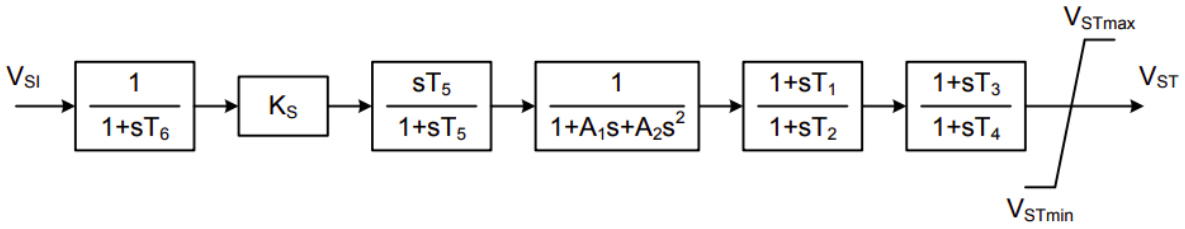

Figure 4.1: Block diagram of the PSS1A stabilizer. [6]

4.1 Non-linear model

Parameters

Table 4.1: Parameters of the Power System Stabilizer

Symbol	Description	Unit
A_1	Notch filter coefficient 1	–
A_2	Notch filter coefficient 2	–
K_s	Stabilizer gain	–
t_1	Lead time constant	s
t_2	Lag time constant	s
t_3	Second lead time constant	s
t_4	Second lag time constant	s
t_5	Washout time constant	s
t_6	Transducer time constant	s
$V_{\text{PSS,max}}$	Maximum stabilizer output limit	pu
$V_{\text{PSS,min}}$	Minimum stabilizer output limit	pu
S_{Nom}	Nominal apparent power	pu

Variables

Table 4.2: Variables of the Power System Stabilizer

Symbol	Description	Unit
ω	Generator speed deviation input	pu
y	Transducer output (filtered speed signal)	pu
y_2	Washout block output	pu
y_3	Notch filter output	pu
y_4	Lead–lag 1 output	pu
y_5	Lead–lag 2 output (before limiter)	pu
V_{PSS}	Stabilizer output voltage signal	pu

$$
\begin{aligned}
t_6\frac{dy}{dt} + y &= \omega \\
t_5\frac{dy_2}{dt} + y_2 &= t_5 K_s y \\
A_2\frac{d^2y_3}{dt^2} + A_1\frac{dy_3}{dt} + y_3 &= y_2 \\
t_2\frac{dy_4}{dt} + y_4 &= t_1\frac{dy_3}{dt} + y_3 \\
t_4\frac{dy_5}{dt} + y_5 &= t_3\frac{dy_4}{dt} + y_4 \\
V_{\text{PSS}} &= \text{sat}(y_5, V_{\text{PSS,min}}, V_{\text{PSS,max}})
\end{aligned}
\tag{4.1}
$$

4.2 Grid Connection Equations

This component is connected to the grid using the following equations:

- ω is an input that comes from the generator's angular speed.
- V_{PSS} is an output that is added to the exciter's voltage reference signal.

4.3 Multi Linear model

The only non multi linear equation in the model is the saturation block at the output. To reformulate it using multi linear equations we use the positive part decomposition:

$$
\begin{aligned}
(y_5 - V_{\text{PSS,min}}) &= u_1 u_2 - v_1 v_2 && (4.2)\\
u_1 u_2 v_1 v_2 &= 0 && (4.3)\\
u_1 - u_2 &= 0 && (4.4)\\
v_1 - v_2 &= 0 && (4.5)\\
& && (4.6)
\end{aligned}
$$

$$(y_5 - V_{\text{PSS,max}}) = u_3 u_4 - v_3 v_4 \tag{4.7}$$
$$u_3 u_4 v_3 v_4 = 0 \tag{4.8}$$
$$u_3 - u_4 = 0 \tag{4.9}$$
$$v_3 - v_4 = 0 \tag{4.10}$$
$$\tag{4.11}$$

$$\text{HardSat}(y_5, V_{\text{PSS,min}}, V_{\text{PSS,max}}) := V_{\text{PSS,min}} + u_1 u_2 - u_3 u_4 \tag{4.12}$$

4.4 Validation

We include the power system stabiliser on top of the governor and exciter. The same simple two-bus system and load variation are used to isolate the effect of the PSSA1. Once again, the responses obtained with the multi-linear model are very similar to those produced by the reference model, demonstrating that the PSS dynamics are captured correctly. We see in 4.2 the previous exciter internal variables as well as the stabilizer's output signal V_{pss}.

Table 4.3: Power System Stabilizer (PSS) Model Parameters

Symbol	Value	Description
		Gain and Limits
K_s	20.0	Stabilizer Gain. Scales the output signal.
$V_{\text{PSS, max}}$	1.0	Maximum stabilizer output limit (pu).
$V_{\text{PSS, min}}$	-1.0	Minimum stabilizer output limit (pu).
		Compensation Time Constants (Lead-Lag/Notch)
T_1	0.02	Lead Time Constant (First stage, s).
T_2	0.1	Lag Time Constant (First stage, s).
T_3	0.02	Lead Time Constant(Second stage, s).
T_4	0.1	Lag Time Constant (Second stage, s).
		Filters and Transducer
T_5	10.0	Washout Time Constant (s).
T_6	0.02	Transducer Time Constant (s)
A_1	1.0	Notch Filter Coefficient 1.
A_2	1.0	Notch Filter Coefficient 2.

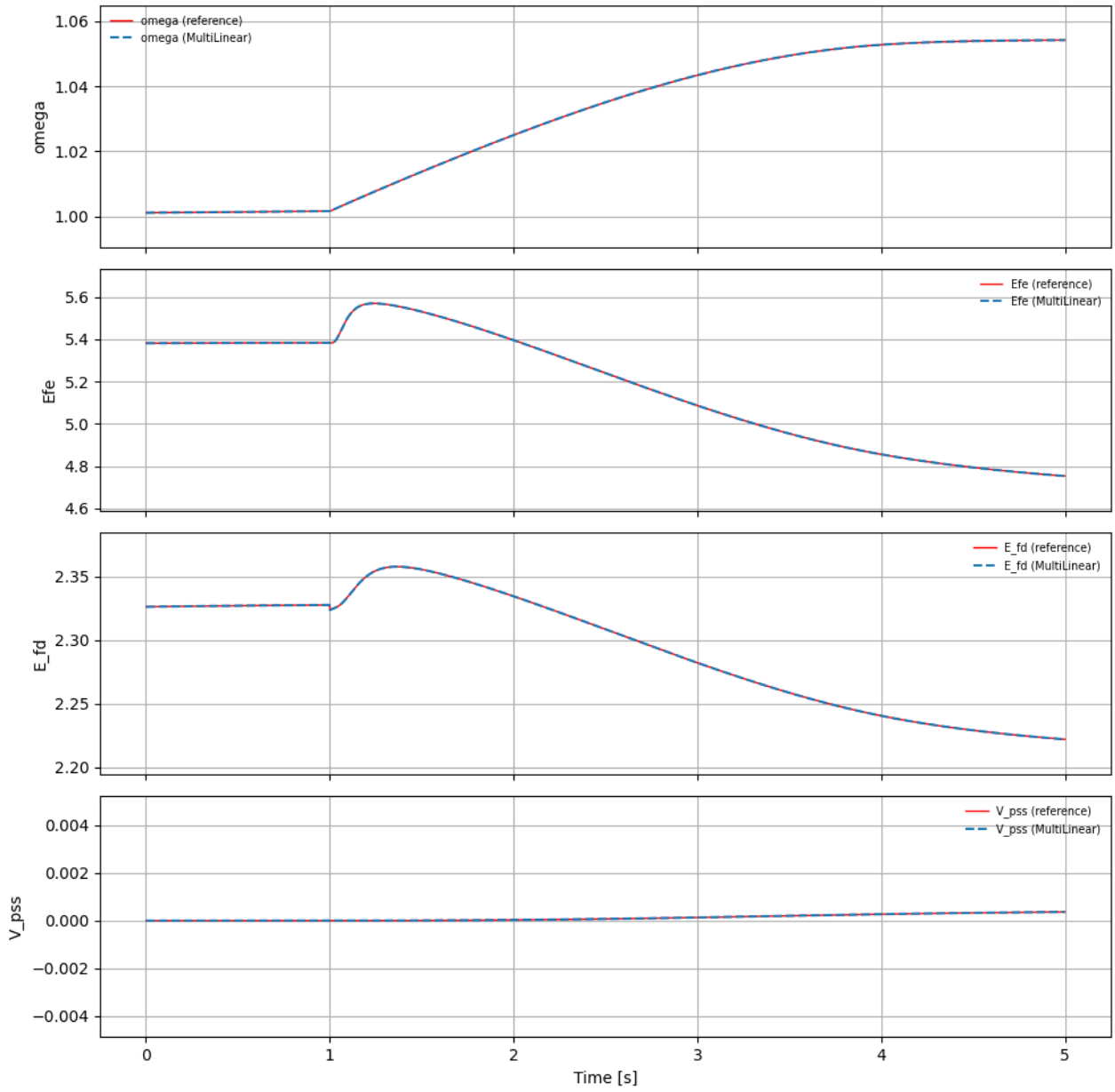

Figure 4.2: Stabilizer Simulation Results Comparison.

5 OEL2C Over excitation limiter

5.1 Non-linear model

The excitation limiter (OEL) supervises the field current or field voltage of the excitation system and prevents over-excitation of the generator under prolonged high reactive power conditions. The model includes current scaling, ramping, and activation/reset logic according to time delays and thresholds, as well as a PID controller that outputs a voltage limiting signal V_{oel}.

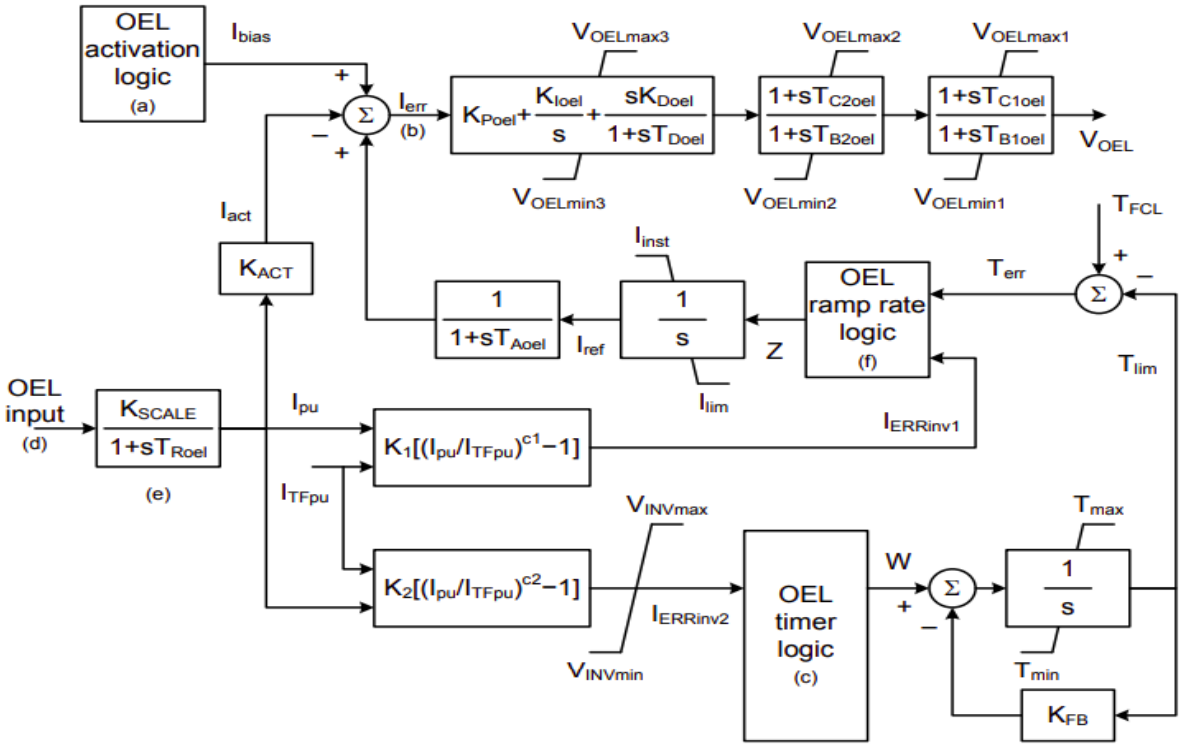

Figure 5.1: Block diagram of the OEL2C over exciter limiter. [6]

Parameters

Table 5.1: Parameters of the Excitation Limiter Model

Symbol	Description	Unit
T_{en}	Enable timer constant	s
T_{off}	Reset timer constant	s
T_{roel}	Current transducer time constant	s
T_{aoel}	Averaging filter time constant	s
T_{doel}	Derivative time constant for PID control	s
T_{min}, T_{max}	Minimum and maximum lag time constants	s
T_{fcl}	Field current limit constant	s
K_{poel}	Proportional gain	–
K_{ioel}	Integral gain	–
K_{doel}	Derivative gain	–
K_{ru}, K_{rd}	Ramp-up and ramp-down gains	–
K_{zru}	Zero ramp-up gain	–
K_{act}	Active current gain	–
K_1, K_2	Inverse characteristic coefficients	–
K_{fb}	Feedback gain	–
K_{scale}	Scaling factor (field rated/base)	–
$I_{\text{tf,pu}}$	Field current per-unit threshold	pu
I_{THoff}	Reset threshold current difference	pu
I_{reset}	Reset bias current	pu
I_{inst}	Instantaneous current limit	pu
I_{lim}	Minimum current limit	pu
$V_{\text{oel,min}}$, $V_{\text{oel,max}}$	Output voltage limits	pu
$V_{\text{inv,min}}$, $V_{\text{inv,max}}$	Inverse characteristic limits	pu
C_1, C_2	Exponent constants for inverse characteristics	–
SW_1	Switch for ramp logic activation	–

Variables

Table 5.2: Variables of the Excitation Limiter Model

Symbol	Description	Unit
E_{fd}	Exciter output voltage (input option)	pu
I_{f}	Field current (input option)	pu
V_{fe}	Field voltage feedback (input option)	pu
I_{pu}	Scaled field current signal	pu
I_{errinv1}, I_{errinv2}	Inverse error signals	pu
W	Logic control signal for ramp logic	pu
T	OEL internal timer variable	s
T_{err}	Timer error signal	pu
I_{a}	Ramp control current	pu
I_{ref}	Current reference signal	pu
I_{act}	Active current signal	pu
I_{bias}	OEL bias control term (activation state)	pu
I_{err}	Error input to PID block	pu
V_{oel}	Limiter output voltage	pu
$V_{\text{oel,sat}}$	Saturated limiter output voltage	pu

5.2 Current Scaling

The first stage converts the selected input signal (field voltage E_{fd}, field current I_f, or exciter feedback voltage V_{fe}) into a per-unit signal on the field winding base:

$$I_{\text{pu}} = \frac{K_{\text{scale}}}{1 + sT_{\text{roel}}} I_{\text{input}} \tag{5.1}$$

where K_{scale} scales the signal from the generator MVA base to the field current base, and T_{roel} represents the small delay of the measurement transducer.

5.3 Inverse Characteristic and Activation Reference

To produce a nonlinear activation behavior, two inverse functions are defined:

$$I_{\text{errinv1}} = K_1 \left[\left(\frac{I_{\text{pu}}}{I_{\text{tf,pu}}} \right)^{C_1} - 1 \right], \qquad I_{\text{errinv2}} = K_2 \left[\left(\frac{I_{\text{pu}}}{I_{\text{tf,pu}}} \right)^{C_2} - 1 \right] \tag{5.2}$$

These functions increase sensitivity when the excitation exceeds its nominal value $I_{\text{tf,pu}}$, creating a smooth transition into the limiting region.

5.4 Timer Logic

The timer logic determines when the OEL should activate or release control. It uses an internal variable T governed by:

$$\frac{dT}{dt} = W - K_{\text{fb}}\,\text{sat}(T, T_{\min}, T_{\max}) \tag{5.3}$$

where

$$W = I_{\text{errinv2}} + H(I_{\text{tf,pu}} - I_{\text{pu}})\,\text{Fixed}_{\text{RU}} + (1 - H(I_{\text{tf,pu}} - I_{\text{pu}}))\,\text{Fixed}_{\text{RD}} \tag{5.4}$$

When the excitation is below the threshold ($I_{\text{pu}} < I_{\text{tf,pu}}$), the fixed ramp-up constant Fixed_{RU} dominates, keeping the timer near zero. When excitation exceeds the threshold, Fixed_{RD} drives T upward, initiating the enable process. The feedback gain K_{fb} limits the timer growth and prevents instability. The timer error

$$T_{\text{err}} = T_{\text{fcl}} - W - K_{\text{fb}} \cdot \text{sat}(T, T_{\min}, T_{\max}) \tag{5.5}$$

is then used as the main signal for enabling and resetting the limiter.

Ramp Logic Once the OEL approaches activation, the ramp logic defines how fast the excitation is reduced. Two ramp slopes are defined:

- K_{ru}: ramp-up coefficient (active when the current is below the limit),
- K_{rd}: ramp-down coefficient (active when the current is above the limit).

The combined slope is given by:

$$C = (1 - \text{SW}_1)K_{\text{ru}} + I_{\text{errinv1}}\text{SW}_1, \tag{5.6}$$

$$D = (1 - \text{SW}_1)K_{\text{rd}} + I_{\text{errinv1}}\text{SW}_1, \tag{5.7}$$

$$Z = C\,\text{Heaviside}(T_{\text{err}} - K_{\text{zru}}T_{\text{fcl}}) + D\,\text{Heaviside}(-T_{\text{err}}) \tag{5.8}$$

which drives the ramp integrator:

$$I_{\text{a}} = \int Z\,dt, \qquad I_{\text{ref}} = \text{sat}(I_{\text{a}}, I_{\text{lim}}, I_{\text{inst}}) \tag{5.9}$$

This ensures a smooth and gradual change of the current reference I_{ref} so that the excitation

reduction is neither abrupt nor oscillatory.

5.5 Bias Signal and Activation Logic

The bias signal I_{bias} determines whether the OEL is actively limiting excitation or not:

- When the enable condition is met, i.e.

$$I_{\text{act}} > I_{\text{ref}} \quad \text{for longer than } T_{\text{en}} \quad \text{or} \quad T_{\text{err}} \leq 0,$$

  the limiter activates and sets:

$$I_{\text{bias}} = 0$$

  meaning the limiter now takes control and prevents any further excitation increase.

- When the reset condition is met, i.e.

$$I_{\text{ref}} = I_{\text{inst}} \quad \text{and} \quad (I_{\text{ref}} - I_{\text{act}}) > I_{\text{THoff}} \quad \text{for longer than } T_{\text{off}},$$

  the limiter releases control and restores the bias to:

$$I_{\text{bias}} = I_{\text{reset}}$$

  re-enabling normal operation of the voltage regulator.

The timers T_{en} and T_{off} ensure the OEL does not toggle rapidly due to transient oscillations or measurement noise.

5.6 PID Control and Output Saturation

The current error applied to the controller is defined as:

$$I_{\text{err}} = I_{\text{ref,avg}} - K_{\text{act}} I_{\text{pu}} + I_{\text{bias}} \tag{5.10}$$

and is processed by a proportional–integral–derivative (PID) control law:

$$V_{\text{oel}} = K_{\text{poel}} I_{\text{err}} + K_{\text{ioel}} \int I_{\text{err}}\, dt + K_{\text{doel}} \frac{dI_{\text{err}}}{dt} \tag{5.11}$$

The limiter output is then constrained within upper and lower bounds:

$$V_{\text{oel,sat}} = \text{Hardsat}(V_{\text{oel}}, V_{\text{oel,min}}, V_{\text{oel,max}}) \tag{5.12}$$

which prevents the limiter from commanding unrealistic voltages.

5.7 Grid Connection

The limiter model takes either the generator field voltage E_{fd} or the exciter fiel current V_{fe} from the exciter and outputs the over exciter limiter voltage value V_{oel} that connects back to the exciter.

5.8 Multilinear model

5.8.1 Heaviside function

We define the Heaviside function as follows. This functions is key to translate the logic depending on the signals into booleans.

Definition 5.8.1. The Heaviside step function is defined as

$$H(x) = \begin{cases} 1, & \text{if } x \geq 0, \\ 0, & \text{if } x < 0. \end{cases}$$

We can multilinearize the Heaviside function by combining the previous use of the multilinear positive and negative parts with an auxiliary variable hv:

$$x^+ := \max(x, 0) \tag{5.13}$$
$$x^- := \max(-x, 0) \tag{5.14}$$
$$x^+ hv = x \tag{5.15}$$

By the last equation we see that if $x^+ = x$ we have that $hv = 1$ and otherwise $hv = 0$. Finally, the full multilinear reformulation yields:

$$u_1 u_2 - v_1 v_2 - xz = 0 \tag{5.16}$$
$$u_1 u_2 v_1 v_2 = 0 \tag{5.17}$$
$$u_1 u_2 hv - x = 0 \tag{5.18}$$
$$u_1 - u_2 = 0 \tag{5.19}$$
$$v_1 - v_2 = 0 \tag{5.20}$$
$$\tag{5.21}$$

5.8.2 Time dependent condition

In this model there is a new kind of non multilinear dependency that is different than the ones seen so far. We express this non multilinear condition in a simpler form first. Let u be an input signal, then the boolean value b is either 1 if $u \geq 0$ for longer than T and 0 otherwise. This dependency is similar to a timer that resets itself whenever a specific condition is not respected. We add an additional state that will be used as a sort of internal clock. The clock works as expected with x reaching the value T only and only if the condition $u \geq 0$ is respected for the preset amount of time and being reset to 0 otherwise, where finally $b \in \mathbb{B}$ the boolean we are looking for:

$$x_0 = 0 \tag{5.22}$$
$$\dot{x} = \begin{cases} 1, & \text{if } x \leq T \text{ and } u \geq 0, \\ -\frac{x}{\Delta t}, & \text{if } x \geq 0 \text{ and } u < 0, \\ 0, & \text{otherwise} \end{cases} \tag{5.23}$$
$$b = (\mathrm{Hv}(x - T - \varepsilon)) \tag{5.24}$$

The previous definition is dependent on Δt and can also be inappropriate for certain solver, we add an auxiliary variable v along a boolean function that forces $(x = 0)$ when the condition is not respected:

$$\dot{x} = \begin{cases} 1, & \text{if } x \leq T \text{ and } u \geq 0, \\ -v, & \text{if } x \geq 0 \text{ and } u < 0, \\ 0, & \text{otherwise} \end{cases} \tag{5.25}$$

$$x\mathrm{Hv}(u) = x \tag{5.26}$$

Finally, we can express this in terms of Heaviside functions:

$$\dot{x} = \mathrm{Hv}(T - x)\mathrm{Hv}(u) - (1 - \mathrm{Hv}(u))\mathrm{Hv}(x)v \tag{5.27}$$

$$x\mathrm{Hv}(u) = x \tag{5.28}$$

In terms of the model, we express the bias activation logic using these equations:

$$\dot{x} = \begin{cases} 1, & \text{if } x \leq T_{\text{en}} \text{ and } I_{\text{act}} - I_{\text{ref}} \geq 0, \\ -v, & \text{if } x \geq 0 \text{ and } I_{\text{act}} - I_{\text{ref}} \leq 0, \\ 0, & \text{otherwise.} \end{cases} \tag{5.29}$$

$$x\mathrm{Hv}(-I_{\text{act}} + I_{\text{ref}}) = x \tag{5.30}$$

Which can be converted to:

$$b_1 = (\mathrm{Hv}(I_{act} - I_{ref})) \tag{5.31}$$

$$b_2 = (\mathrm{Hv}(-T_{err})) \tag{5.32}$$

$$b_3 = b_1 + b_2 - b_1 b_2 \tag{5.33}$$

$$\dot{x} = \mathrm{Hv}(T_{en} - x)b_3 - (1 - b_3)\mathrm{Hv}(x)(-v) \tag{5.34}$$

$$x = x\mathrm{Hv}(1 - b_3) \tag{5.35}$$

Now we define the timer boolean for the other boolean condition and we get:

$$b_4 = \mathrm{Hv}(I_{ref} - I_{inst})\mathrm{Hv}(-I_{inst} + I_ref) \quad (5.36)$$
$$b_5 = \mathrm{Hv}(I_{\mathrm{ref}} + I_{\mathrm{act}} - I_{\mathrm{THoff}}) \quad (5.37)$$
$$b_6 = b_4 b_5 \quad (5.38)$$
$$\dot{y} = \mathrm{Hv}(T_{off} - y)b_6 - (1 - b_6)\mathrm{Hv}(y)(-v_y) \quad (5.39)$$
$$\dot{x} = \mathrm{Hv}(T_{en} - x)b_3 - (1 - b_3)\mathrm{Hv}(x)(-v) \quad (5.40)$$
$$x = x(1 - \mathrm{Hv}(I_{\mathrm{act}} - I_{\mathrm{ref}})) \quad (5.41)$$
$$y = y(1 - \mathrm{Hv}(1 - b_6)) \quad (5.42)$$

Now we can express the different conditions in boolean algebra:

$$c_1 = \mathrm{Hv}(T_{off} - x - \varepsilon) \quad (5.43)$$
$$c_2 = \mathrm{Hv}(T_{en} - y - \varepsilon) \quad (5.44)$$
$$(5.45)$$

We can finally express I_{bias} as:

$$I_{bias} = c_1(1 - c_2)I_{reset} \quad (5.46)$$

5.8.3 Timer Logic multilinear expression

The timer logic is more straight forward as it can expressed with a Heaviside function.

$$W = \mathrm{Hv}(I_{Fpu} - I_{pu}) \times (\mathrm{Fixed}_{RU} + I_{ERRinv2}) + (1 - \mathrm{Hv}(I_{Fpu} - I_{pu})) * (\mathrm{Fixed}_{RD} + I_{ERRinv2}) \quad (5.47)$$

5.8.4 Ramp Logic

The ramp logic uses user selected parameters to select the ramp rate. Particularly SW_1 is a switch value selected by the user that belongs to the interval $\{0, 1\}$.

$$C = (1 - SW_1)\, K_{ru} + I_{\text{errinv1}}\, SW_1, \tag{5.48}$$

$$D = (1 - SW_1)\, K_{rd} + I_{\text{errinv1}}\, SW_1, \tag{5.49}$$

$$Z = C \cdot \mathrm{Hv}(T_{\text{err}} - K_{zru}\, T_{fcl}) + D \cdot \mathrm{Hv}(-T_{\text{err}}). \tag{5.50}$$

6 Grid Following Converter

This model represents the behavior of a Grid following controller. It departs from the previous models in that it considers the three phases of the grid separately instead of the phasor values. This difference arises from the use of Electro Magnetic Transient types of models that are more sensible to specific changes in values.

The converter functions as a precise current source that is entirely dependent on the grid: it uses a Phase-Locked Loop (PLL) to accurately estimate the instantaneous grid angle (θ) and frequency. This angle is crucial for aligning the converter's internal reference frame, allowing the inner current control loop to precisely determine and inject the required current components

(i_d) and reactive (i_q) into the network, thereby ensuring synchronization and managing terminal voltage under rapid fault conditions.

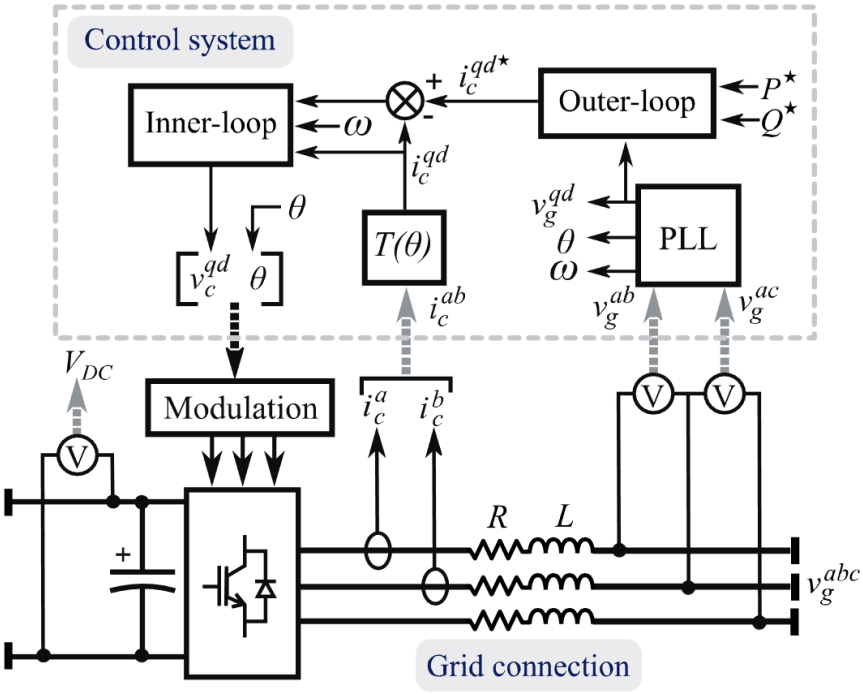

Figure 6.1: Block diagram of the GFL converter model. [7]

Variables

Table 6.1: List of variables used in the converter model.

Symbol	Description	Unit
$x_{a,b,c}$	Instantaneous phase quantities (a, b, c)	–
X	Signal amplitude	–
θ	Grid voltage phase angle	rad
$\hat{\theta}$	Estimated grid angle (PLL output)	rad
δ	Angle error $\theta - \hat{\theta}$	rad
v^d, v^q	Converter voltages in dq frame	V
v_g^{qd}	Grid voltage in dq frame	V
v_c^{qd}	Converter internal voltage reference in dq frame	V
i^d, i^q	Converter currents in dq frame	A
i^{d*}, i^{q*}	Current reference signals in dq frame	A
E_m	Magnitude of grid voltage vector	V
ω	Instantaneous angular frequency	rad/s
P, Q	Active and reactive power	W, var
P^*, Q^*	Active and reactive power setpoints	W, var
$\hat{P}$	Measured active power	W
S	Apparent power	VA
v^{abc}	Three-phase voltage vector	V
i^{abc}	Three-phase current vector	A
E^{qd}	Current control error signal	A
V_c^{qd}	PI controller output voltage reference	V
t	Time	s
s	Laplace variable	–

Parameters

Table 6.2: List of parameters used in the converter model.

Symbol	Description	Unit
K_p^{pll}	Proportional gain of PLL controller	–
K_i^{pll}	Integral gain of PLL controller	–
K_p^{icl}	Proportional gain of current controller	–
K_i^{icl}	Integral gain of current controller	–
K_p^{pol}	Proportional gain of power controller	–
K_i^{pol}	Integral gain of power controller	–
R	Filter or line resistance	Ω
L	Filter or line inductance	H
ω_s	Synchronous angular speed of the grid	rad/s
τ_c	Power control filter time constant	s
V_{peak}	Peak value of the grid voltage	V

6.1 Non-linear model

6.1.1 Phased Locked Loop

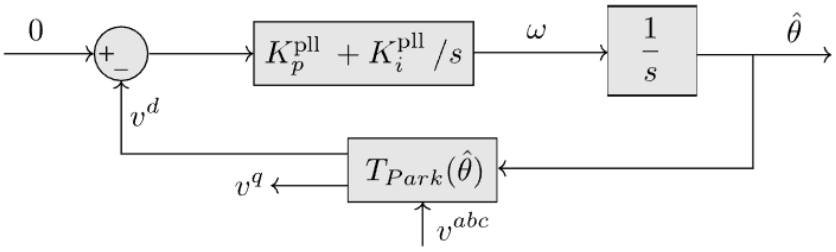

Figure 6.2: Block diagram of the PLL controller.

The phase locked loop is a controller that takes the three voltage phases v_a, v_b, v_c and outputs an estimated angle $\hat{\theta}$. The PLL works by trying to align v^d to 0. To properly model the PLL we first transform the voltage values in the a, b, c coordinates to d, q coordinates. We use the Park Transform, expressed in the following equations:

$$v_d = \frac{1}{3}\Big(2\cos\theta\, v_a + (-\cos\theta - \sqrt{3}\sin\theta)\, v_b + (-\cos\theta + \sqrt{3}\sin\theta)\, v_c\Big) \tag{6.1}$$

$$v_q = \frac{1}{3}\Big(2\sin\theta\, v_a + (-\sin\theta + \sqrt{3}\cos\theta)\, v_b + (-\sin\theta - \sqrt{3}\cos\theta)\, v_c\Big) \tag{6.2}$$

$$\omega = K_p\, v_d + K_i \int v_d\, dt \tag{6.3}$$

$$\theta = \int \omega\, dt \tag{6.4}$$

6.1.2 Current Control

The current control is used to determine the converter voltage that has to be applied in order to maintain the current at the setpoint. The model presented uses the Internal Model Control that uses the relationship between voltages and currents:

$$v_c^{qd} - v_g^{qd} = \begin{bmatrix} R & L\omega \\ -L\omega & R \end{bmatrix} i_c^{qd} + L\frac{d\, i_c^{qd}}{dt} \tag{6.5}$$

The control diagram associated with the equation has coupling between the d and q axes. Given the set points $\hat{v}^q$, $\hat{v}^d$ the final voltage values are:

$$v_c^d = K_p\,(i^{d*} - i_d) + K_i \int (i^{d*} - i_d)\, dt + v_d + L\,\omega\, i_q \tag{6.6}$$

$$v_c^q = K_p\,(i^{q*} - i_q) + K_i \int (i^{q*} - i_q)\, dt + v_q - L\,\omega\, i_d \tag{6.7}$$

These equation define a set of two PI controllers that define the value of the d,q voltages depending of the error signal $i^{d*} - i^d$ and $i^{q*} - i^q$.

6.1.3 Power Control Loop

We obtain the active and reactive power values with these formula:

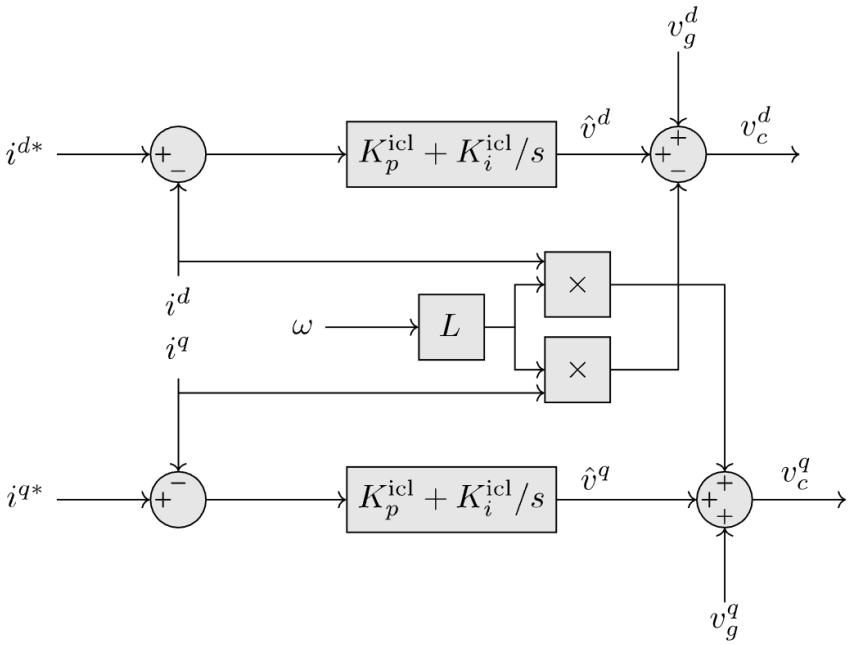

Figure 6.3: Block diagram of the current control block. [8]

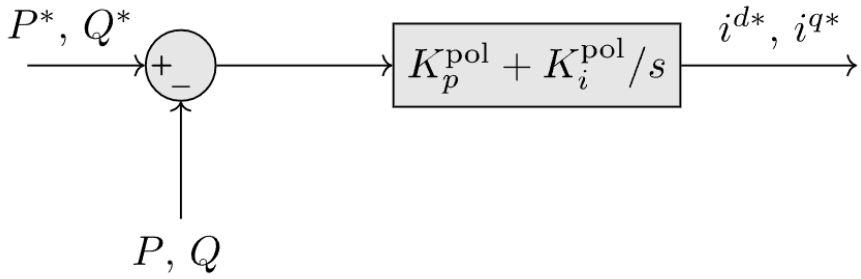

Figure 6.4: Power control diagram.[8]

$$P = \frac{3}{2}\left(v^q i^q + v^d i^d\right), \tag{6.8}$$

$$Q = \frac{3}{2}\left(v^q i^d - v^d i^q\right). \tag{6.9}$$

And we control the value of the intensity's set points with the PI:

$$i^{d*} = K_p^Q \left(Q^* - Q\right) + K_i^Q \int \left(Q^* - Q\right) dt \tag{6.10}$$

$$i^{q*} = K_p^P \left(P^* - P\right) + K_i^P \int \left(P^* - P\right) dt \tag{6.11}$$

6.2 Physical Limitation

To determine the saturation limits of the current components, the operation mode of the converter must be taken into account, since it dictates which current component shall be prioritised. These operation modes are typically established in the grid codes, although a representative implementation can be described as follows.

In normal operation, the converter prioritises the tracking of the active power related current component, in this case the intensity's q axis component. The remaining current component is then saturated according to the converter capability,

$$i_d^2 + i_q^2 \leq I_{\max}^2,$$

so that the commanded current vector remains inside the permissible current circle.

During grid disturbances, the converter modifies its priority and gives precedence to the current component associated with voltage support. In this case the d component.

For normal operations the equations defining the saturation are the following:

$$i_{d,\max} = \sqrt{\max(I_{\max}^2 - \max(i_q,\, i_{q,\mathrm{ref}})^2,\, \varepsilon)} \tag{6.12}$$

$$i_{d,\mathrm{ref}} = \mathrm{Hardsat}(i_{d,\mathrm{ref}},\, -i_{d,\max},\, i_{d,\max}) \tag{6.13}$$

$$i_{q,\mathrm{ref}} = \mathrm{Hardsat}(i_{q,\mathrm{ref}},\, -I_{\max},\, I_{\max}) \tag{6.14}$$

6.3 Modulation

The modulation inside the converter takes the set point values from the control blocks and outputs a physical electric signal that follows the setpoints. The converter uses IGBT pulses to

generate the electric wave. For the sake of simplicity, we define that the output signal is directly equal to the set points values.

6.4 Multilinear Model

The model non multilinear equations are related to the use of the $\sin$ and $\cos$ functions. We multilinearize this functions by using the following reformulation, in this case we apply the reformulation exclusively for $\cos(\theta)$ and $\sin(\theta)$.To obtain the multilinearization we apply the ideas present in [9], particularly for multi linearization of the PLL and Park transformation. .

$$u^{\cos} := \cos(\theta) \tag{6.15}$$

$$u^{\sin} := \sin(\theta) \tag{6.16}$$

$$\frac{\partial u^{\cos}}{\partial t} = -u^{\sin}\frac{\partial \theta}{\partial t} \tag{6.17}$$

$$\frac{\partial u^{\sin}}{\partial t} = u^{\cos}\frac{\partial \theta}{\partial t} \tag{6.18}$$

The transfer functions used in the multiple PID controllers are already multilinear and can be expressed in the time domain as follows, where $u(t)$ the input, $x(t)$ an internal state and $y_i(t)$ the output.

$$\dot{x}_i(t) = u_i(t), \tag{6.19}$$

$$y_i(t) = K_{p,i}\, u_i(t) + K_{i,i}\, x_i(t) + K_{d,i}\, \dot{u}_i(t), \quad i = 1, 2, \ldots, n \tag{6.20}$$

6.5 Grid Connection & Validation

This model differs from the rest of the models in that it is connected to the grid in two points. To a DC bus on one side and to a 3 phase line on the other. We use three different buses with coupled singled-phased system to recreate the three phases in AC connection.

The resistance and inductances connected to the converter yield the following circuit equations:

$$v_{a,\text{conv}} - v_{ag} = R\, i_g^a + L\, \frac{\partial i_g^a}{\partial t} \tag{6.21}$$

$$v_{b,\text{conv}} - v_{bg} = R\, i_g^b + L\, \frac{\partial i_g^b}{\partial t} \tag{6.22}$$

$$v_{c,\text{conv}} - v_{cg} = R\, i_g^c + L\, \frac{\partial i_g^b}{\partial t} \tag{6.23}$$

Additionally, we also consider an ideal voltage source at the grid connection v_g^{abc} this fixes the values of the voltages:

$$v_a(t) = \cos(\omega_{\text{base}}\, t), \tag{6.24}$$

$$v_b(t) = \cos\left(\omega_{\text{base}}\, t - \tfrac{2\pi}{3}\right), \tag{6.25}$$

$$v_c(t) = \cos\left(\omega_{\text{base}}\, t + \tfrac{2\pi}{3}\right). \tag{6.26}$$

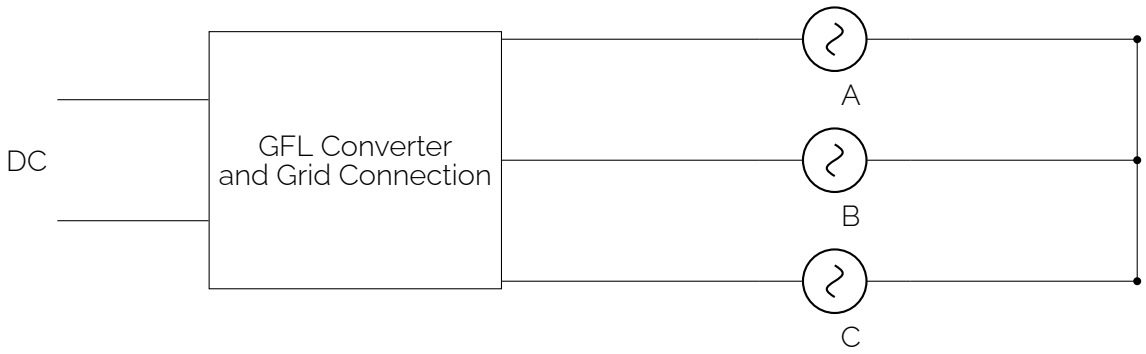

Figure 6.5: Validation Setup for GFL converter.

To validate this setup, we initialise the system from a cold start, that is, all internal states of the converter and the network begin from zero or nominal initial conditions without any pre-computed operating point until it reaches a steady state. This steady state is then taken as the initial point of the simuation and is chosen arbitrarily. The simulation is then run for $0.5\,\text{s}$ using a fixed timestep of $10^{-4}\,\text{s}$, which is sufficiently small to capture the EMT dynamics of the GFL model and to ensure that the trigonometric transformations remain accurate. We compare the trajectories obtained with the reference model and with the multilinear formulation. In particular, we examine the converter-side phase voltages and the trigonometric reformulations used in the PLL and current control blocks. In all cases, the two implementations yield very similar time series, confirming that the multilinear representation reproduces the behaviour of the original

Table 6.3: Grid-Following Converter (GFL) Model Parameters

Symbol	Value	Description
General System and Component Parameters		
R	0.1	Filter/Coupling Resistance (pu).
L	0.01	Filter/Coupling Inductance (pu).
V_{peak}	325.0	Peak DC-link voltage limit (example, V).
V_{dc}	100	DC-link voltage source (V).
$I_{\max}$	1.2	Maximum instantaneous current limit (pu).
P_{ref}	1.0	Active Power reference (pu).
Q_{ref}	0.1	Reactive Power reference (pu).
Phase-Locked Loop (PLL) Parameters		
$K_{p,\text{PLL}}$	0.001	PLL Proportional Gain.
$K_{i,\text{PLL}}$	0.1	PLL Integral Gain.
ω_{nom}	$2\pi \cdot 50$	Nominal angular frequency (rad/s).
Outer Power Control Loop (POL) Parameters		
$K_{p,\text{POL}}$	0.05	Power Outer Loop Proportional Gain.
$K_{i,\text{POL}}$	1.0	Power Outer Loop Integral Gain.
Inner Current Control Loop (ICL) Parameters		
$K_{p,\text{ICL}}$	0.05	Current Inner Loop Proportional Gain.
$K_{i,\text{ICL}}$	1.0	Current Inner Loop Integral Gain.

model with numerical accuracy.

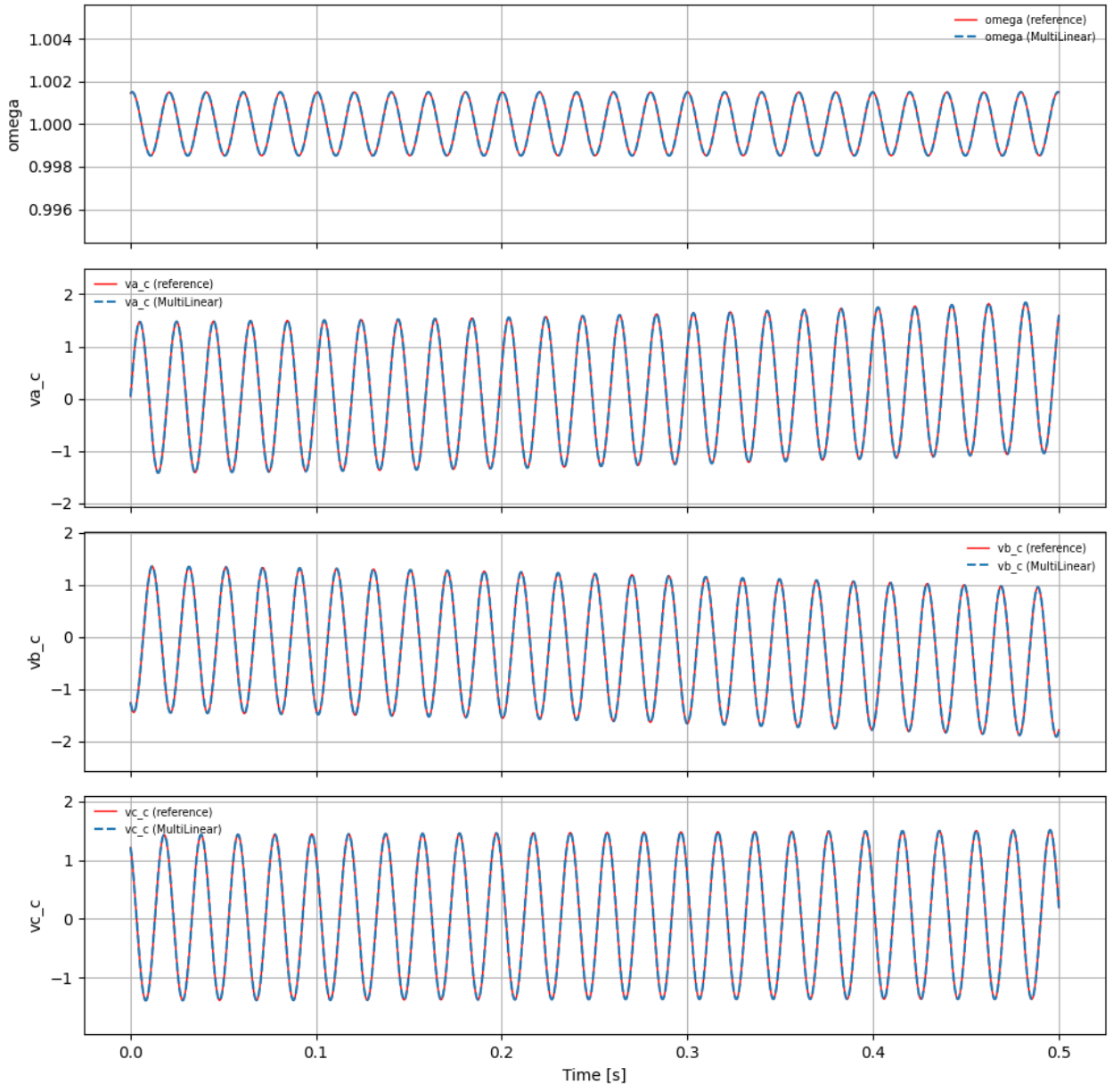

Figure 6.6: Converter side voltages results comparison.

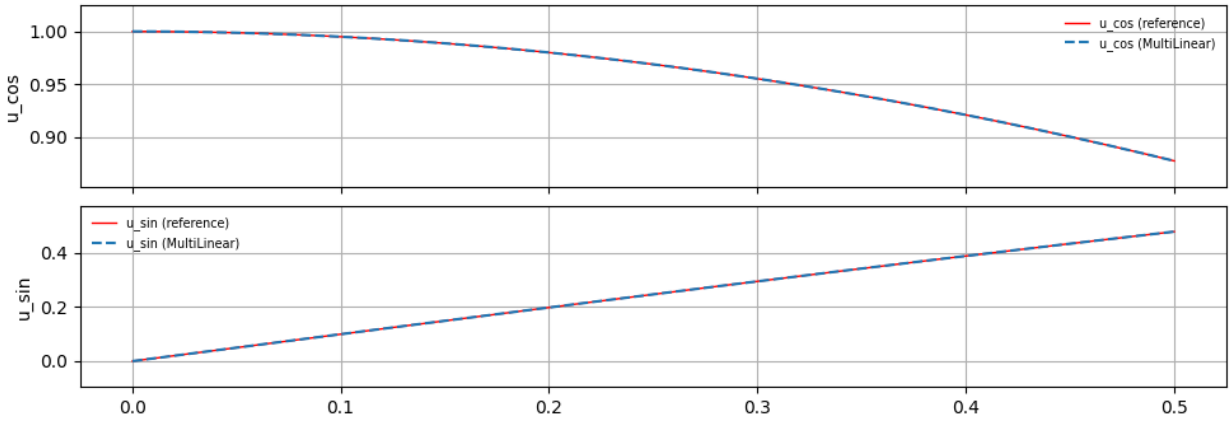

Figure 6.7: Trigonometric variables results comparison.

7 Grid Forming Converter

This model represents a Grid Forming converter. Grid-forming converters operate as voltage sources that establish and regulate the grid voltage and frequency. They are capable of setting the reference for other devices. In contrast, grid-following converters behave as current sources that synchronize to an existing grid voltage through a phase-locked loop (PLL). Their operation depends on an external voltage reference, making them suitable for strong grids where the voltage and frequency are already defined by other sources.

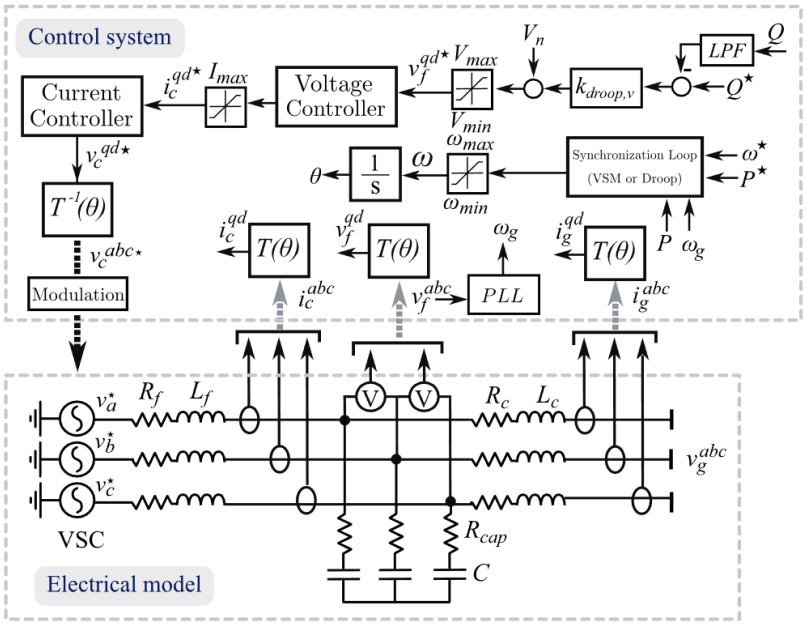

Figure 7.1: Block diagram of the GFM converter model. [7]

Variables

Table 7.1: Variables of the grid-forming converter model. [7]

Symbol	Description
ω	Instantaneous converter angular frequency (rad/s)
ω^*	Reference angular frequency (rad/s)
$\Delta\omega$	Frequency deviation from reference (rad/s)
P, Q	Active and reactive power (W, var)
P^*, Q^*	Reference active and reactive power (W, var)
V, V^*	Converter voltage magnitude and reference (V)
ΔP, ΔQ	Power deviations from reference (W, var)
θ	Converter voltage angle (rad)
v_f^d, v_f^q	Filter capacitor voltages in dq frame (V)
v_c^d, v_c^q	Converter output voltages in dq frame (V)
v_g^d, v_g^q	Grid voltages in dq frame (V)
i_c^d, i_c^q	Converter currents in dq frame (A)
i_g^d, i_g^q	Grid currents in dq frame (A)
i_f^d, i_f^q	Filter current components in dq frame (A)
$\hat{i}_c^{qd*}$	Estimated converter current reference (A)
$\hat{v}^d$, $\hat{v}^q$	Estimated control voltages (V)

Parameters

Table 7.2: Parameters of the grid-forming converter model.

Symbol	Description
$K_{\Delta P}$, $K_{\Delta Q}$	Droop control coefficients for frequency and voltage
$\tau_{\Delta P}$	Time constant of the frequency droop filter (s)
C_f	Filter capacitance (F)
L_f, L_c	Filter and coupling inductances (H)
R_f, R_c	Filter and coupling resistances (Ω)
K_p^{vcl}, K_i^{vcl}	Voltage control proportional and integral gains
K_p^{icl}, K_i^{icl}	Current control proportional and integral gains
ω_s	Synchronous angular frequency (rad/s)
$G_c(s)$	Current control transfer function

7.1 Non multilinear Model

The Synchronization method defines the angle and voltage magnitude that the converter will use to operate. In this work we explore two models, the Virtual Synchronous Machine (VSC) and the Droop control. The droop control is a special case of the VSC control.

7.1.1 Droop Control

In the droop control we consider a reference value for the grid frequency ω^* (usually 50 Hz) and a reference power P^*. The droop control first passes the power signal (P or Q)through a low pass filter and then subtracts it from the reference value to obtain the filtered power deviation. Finally, the resulting frequency value is linearly dependent on ΔP around ω^*. More specifically:

$$\omega = \omega^* - K_{\Delta P}(\hat{P} - P^*) \tag{7.1}$$

Similarly for the voltage control we have that:

$$V = V^* - K_{\Delta Q}(\hat{Q} - Q^*) \tag{7.2}$$

Where both $\hat{P}$ and $\hat{Q}$ are the outputs of the respective low pass filters.

$$E_P(s) = P^*(s) - \hat{P}(s), \tag{7.3}$$

$$\hat{P}(s) = \frac{1}{s\tau_{\Delta P} + 1} P(s), \tag{7.4}$$

$$\Delta\omega(s) = K_{\Delta P}\, E_P(s), \tag{7.5}$$

$$\omega(s) = \omega^*(s) + \Delta\omega(s), \tag{7.6}$$

$$\theta(s) = \frac{1}{s}\omega(s) \tag{7.7}$$

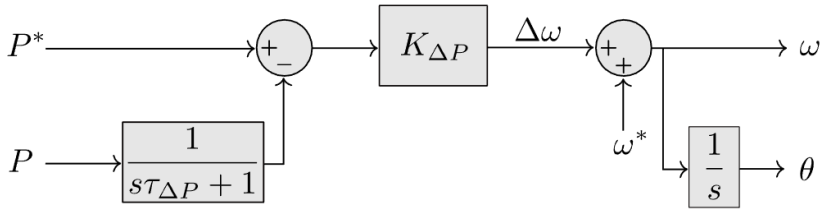

Figure 7.2: Block diagram of the frequency control.

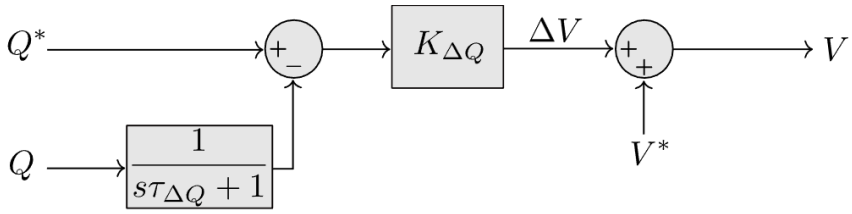

Figure 7.3: Block diagram of the voltage magnitude control. [8]

7.1.2 VSC Loop

7.1.3 Voltage Control

The converter determines the set points values i_d^*, i_q^* with the control loop. We use the following circuit equation to find the appropriate control, where C_f is the capacitance of the filter (one of the converter's parameter) and i_g^{qd} the observed current measurements at the grid.

$$\hat{i}_c^{qd*} - i_g^{qd} = \begin{bmatrix} 0 & -\omega C_f \\ \omega C_f & 0 \end{bmatrix} \begin{bmatrix} v_f^{qd} \\ v_f^q \end{bmatrix} + \frac{d}{dt} \begin{bmatrix} v_f^d \\ v_f^q \end{bmatrix} \tag{7.8}$$

We can use a change of variable and a Laplace transformation to find the following equation:

$$\begin{bmatrix} i^d \\ i^q \end{bmatrix} = \begin{bmatrix} i_c^d - i_g^d + \omega C_f v_f^q \\ i_c^q - i_g^q - \omega C_f v_f^d \end{bmatrix} = \begin{bmatrix} sC_f v_f^d \\ sC_f v_f^q \end{bmatrix} \tag{7.9}$$

The final current values are:

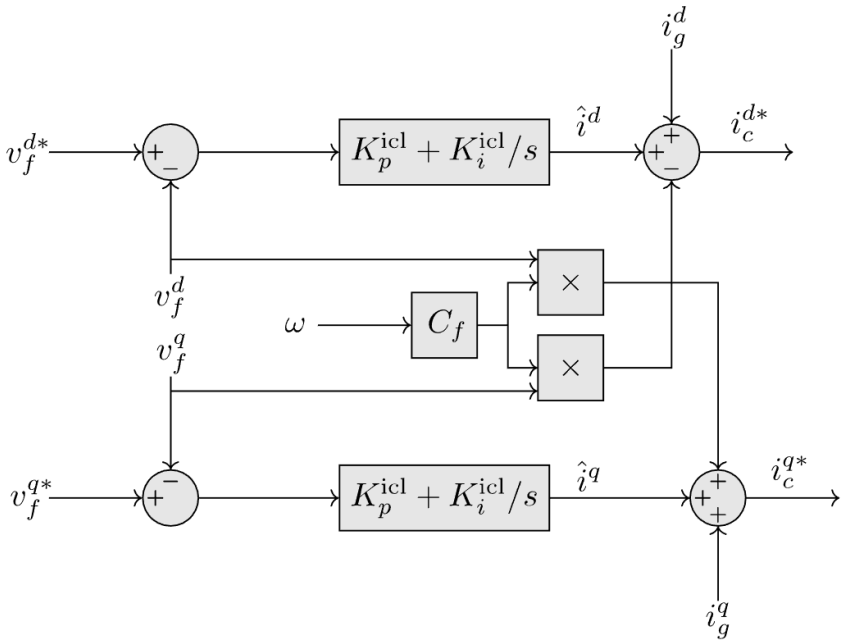

Figure 7.4: Block diagram of the voltage control loop. [8]

$$i_c^d = K_p\,(v^{d*} - v_d) + K_i \int (v^{d*} - v_d)\,dt + i_d + C_f\,\omega\,v_q \tag{7.10}$$

$$i_c^q = K_p\,(v^{q*} - v_q) + K_i \int (v^{q*} - v_q)\,dt + i_q - C_f\,\omega\,v_d \tag{7.11}$$

7.1.4 Current Control

The current control in the GFM converter is very similar to the one in the GFL converter, we begin with the equation describing the electrical connection circuit expressed in the dq frame:

$$v_c^{qd*} - v_f^{qd} = \begin{bmatrix} R_f & L_f\omega \\ -L_f\omega & R_f \end{bmatrix} i_c^{qd} + L_f \frac{d}{dt} i_c^{qd} \tag{7.12}$$

The control diagram associated with the equation has coupling between the d and q axes. Final voltage values are:

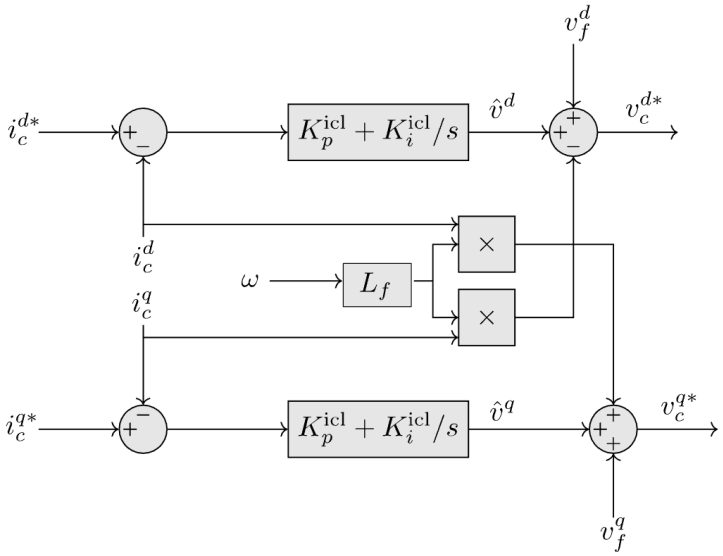

Figure 7.5: Block diagram of the current control loop. [8]

$$v_c^d = K_p\,(i^{d*} - i_d) + K_i \int (i^{d*} - i_d)\,dt + v_d + L\,\omega\,i_q \tag{7.13}$$

$$v_c^q = K_p\,(i^{q*} - i_q) + K_i \int (i^{q*} - i_q)\,dt + v_q - L\,\omega\,i_d \tag{7.14}$$

Similarly to the GFL converter we can decouple the loop control. We then find the equation:

$$\begin{bmatrix} \hat{v}^q \\ \hat{v}^d \end{bmatrix} = \begin{bmatrix} R_f & 0 \\ 0 & R_f \end{bmatrix} \begin{bmatrix} i_c^q \\ i_c^d \end{bmatrix} + L_f \frac{d}{dt} \begin{bmatrix} i_c^q \\ i_c^d \end{bmatrix} \tag{7.15}$$

7.2 Physical Limitations & Validation

We use the same current limitation as in the GFL converter. Additionally, we also consider a voltage limitation for the voltage values where we rescale the d, q voltages values of the converter with respect to a V_{max}:

$$\rho = \min(1, \frac{V_{max}}{\sqrt{(v^d_{ref})^2 + (v^q_{ref})^2}}) \tag{7.16}$$

$$v^d_{ref,sat} = \rho v^d_{ref} \tag{7.17}$$

$$v^q_{ref,sat} = \rho v^q_{ref} \tag{7.18}$$

7.3 Multilinear Model

We reformulate the trigonometric functions in the same way as in the GFM converter however here we also have to deal with the minimum function. To obtain the multilinearization we apply the ideas present in [9], particularly for multi linearization of the PLL and Park transformation.

7.3.1 Min function

We first formulate the minimum function as a sum of expressions which we already know how to multilinearize, in this case the positive part. The following equation can easily be verified separating by cases:

$$(x-y)^+ := \max(x-y, 0) \tag{7.19}$$

$$\min(x, y) = x - (x-y)^+ \tag{7.20}$$

The previous multilinear expressions of the positive and negative were ill-conditioned for this particular model, so we use a more compact formulation for the positive part specifically. Let A a linear expression then the following equations define three auxiliary variables were $w = max(A, 0)$.

$$u_+ - v_+ = 0, \tag{7.21}$$

$$u_+ \, v_+ - w = 0, \tag{7.22}$$

$$u_+ \, v_+ \, w - wA = 0. \tag{7.23}$$

This can be seen because 7.23 forces $w \geq 0$ since w is equal to u_+ squared, and the final equation forces w to be 0 if A is negative and if A is positive we can divide by w which forces $A = u_+ \, v_+ =$

w.

With this we can define ρ as a correcting parameter for v^d_{ref}, and v^d_{ref}:

$$u^{aux}u_2^{aux}(v^d_{ref}v^d_{ref,aux}) + (v^q_{ref}v^q_{ref,aux}) = V^2_{max} \tag{7.24}$$
$$u^{aux} = u_2^{aux} \tag{7.25}$$
$$v^d_{ref} = v^d_{ref,aux} \tag{7.26}$$
$$v^q_{ref} = v^q_{ref,aux} \tag{7.27}$$
$$\rho = 1 - (u_{aux} - 1)^+ \tag{7.28}$$
$$\tag{7.29}$$

$$\rho v^d_{ref} = v^d_{ref,sat} \tag{7.30}$$
$$\rho v^q_{ref} = v^q_{ref,sat} \tag{7.31}$$
$$\tag{7.32}$$

7.4 Grid Connection & Validation

We follow the connection scheme in 7.1, and we add to the AC side three resistances in parallel that are connected to the ground. The DC is considered fixed and doesn't interact with the converter in the simulation.

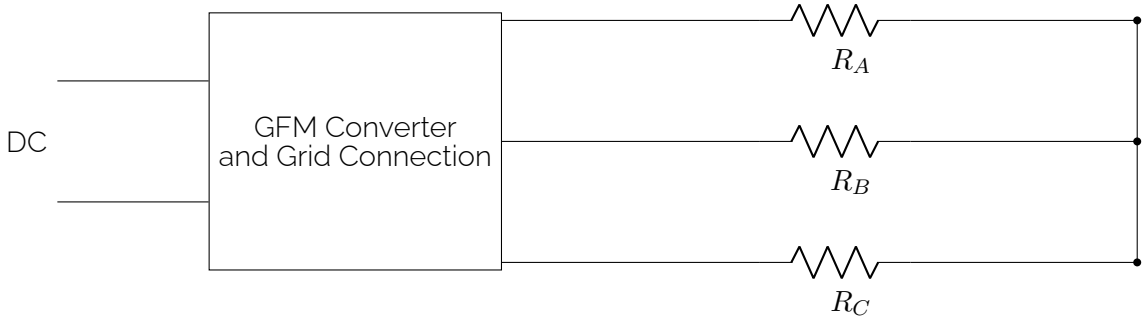

Figure 7.6: Validation Setup for GFM converter.

For the grid-forming converter, we follow a similar validation procedure to the GFL converter. The system is initialized from a cold start, meaning that all dynamic states of the converter controller, the virtual oscillator, and the network begin from zero or nominal default values without

enforcing a pre-defined steady-state and run the simulation until a steady state is found. The simulation is then executed for $0.5\,\mathrm{s}$ with a fixed timestep of $10^{-4}\,\mathrm{s}$. We compare the results of the reference implementation with those of the multilinear model by inspecting the converter terminal voltages (${v_d^{ref}}_c, {v_q^{ref}}_c$) and the auxiliary trigonometric variables that appear in the grid-forming control structure. As in the GFL case, both models exhibit identical trajectories throughout the entire simulation, confirming that the multilinear formulation accurately reproduces the behavior of the original grid-forming converter.

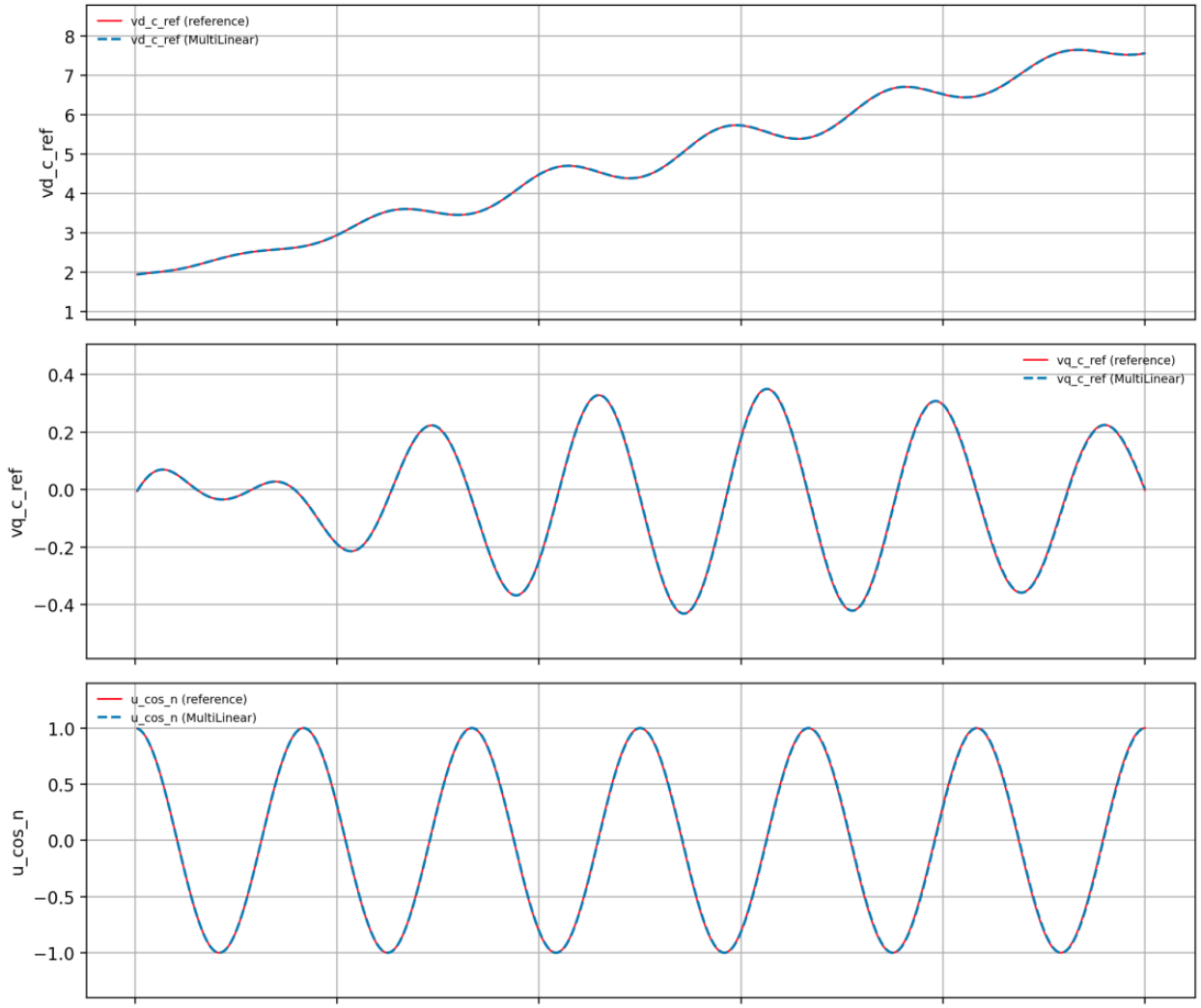

Figure 7.7: Simulation Results Comparison of the GFM converter Simulation.

Table 7.3: Grid-Forming Converter (GFM) and LCL Filter Parameters

Symbol	Value	Description
		LCL Filter Parameters (Coupling Network)
R_f	0.02	Resistance of the Converter-side Inductor L_f (pu).
L_f	0.15	Inductance of the Converter-side Inductor (pu).
R_c	0.01	Resistance of the Grid-side Inductor L_c (pu).
L_c	0.05	Inductance of the Grid-side Inductor (pu).
C_f	0.05	Capacitance of the Filter Capacitor (pu).
R_{cap}	10.0	Capacitor damping resistance (pu).
R_{load}	1.0	Per-phase resistance of the external load (pu).
		GFM Synchronizing and Reference Parameters
K_{dp}	0.02	ω-P Droop Gain (Frequency vs. Active Power).
K_{dq}	0.05	V-Q Droop Gain (Voltage vs. Reactive Power).
ω_{ref}	1.0	Reference angular speed (pu).
ω_{nom}	$2\pi \cdot 50$	Nominal angular frequency (rad/s).
V_{ref}	1.0	Nominal voltage magnitude reference (pu).
$V_{\max}$	1.1	Maximum voltage output limit (pu).
$I_{\max}$	1.2	Maximum current output limit (pu).
P_{ref}	10	Active Power reference for droop steady-state (pu).
Q_{ref}	0.1	Reactive Power reference for droop steady-state (pu).
		GFM Control Loop and Filtering Parameters
$K_{p,\text{ICL}}$	0.05	Inner Current Control Loop Proportional Gain.
$K_{i,\text{ICL}}$	50.0	Inner Current Control Loop Integral Gain.
τ_P	0.01	Low-pass filter time constant for Active Power (s).
τ_Q	0.01	Low-pass filter time constant for Reactive Power (s).

7.5 Conclusion

7.6 Conclusion

This work has established a modeling framework suitable for the stability analysis of modern, hybrid power systems. On the conventional generation side, a detailed synchronous machine model (**GenQEC**) was implemented, incorporating quadratic saturation to accurately capture magnetic non-linearities. This generator is coupled with industry-standard control systems, including the AC1C excitation system, the IEEEG1 steam governor, the PSS1A power system stabilizer and the OELC2 over excitation limiter. The choice of models respond to a need of simulating

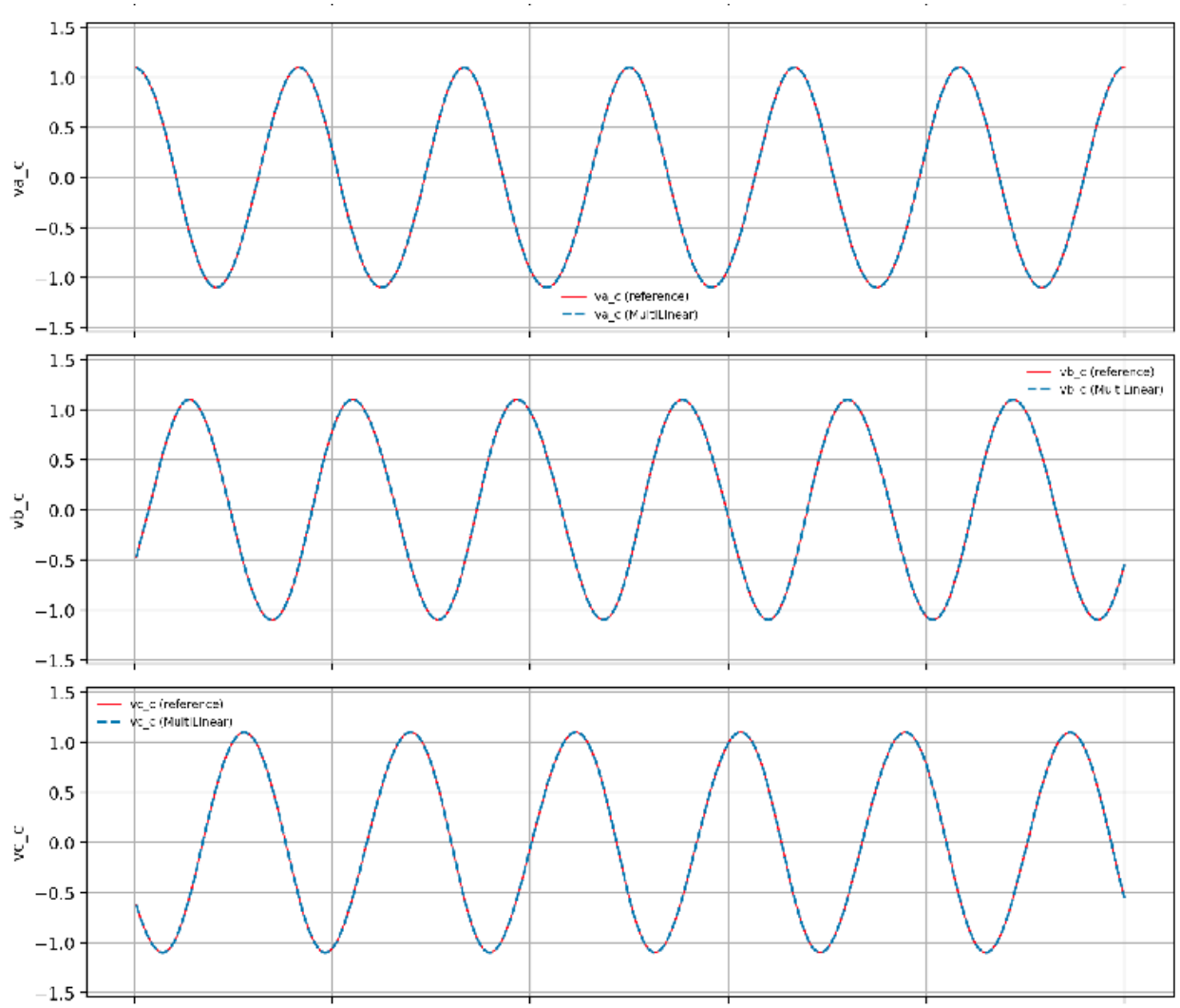

Figure 7.8: Simulation Results Comparison for GFM converter.

standard industry models that include all the different components and control systems that can be present in traditional power generation.

To address the importance , the system model was expanded to include detailed representations of Inverter-Based Resources (IBRs). Both Grid-Following (GFL) and Grid-Forming (GFM) converters were modeled using three-phase instantaneous variables rather than simplified phasors. These models explicitly account for the fast dynamics of Phase-Locked Loops (PLL), inner current control loops, and LCL filter interactions, providing the necessary detail for analyzing electromagnetic transients.

A central contribution of this modeling approach is the application of multilinear modeling. By systematically approximating non-linear behaviors such as magnetic saturation, division in power

calculation, and trigonometric frame transformations into a multilinear structure, this framework enables the use of based tools. The future objective is to then integrate these models with the tensor based tools developped in the framework of the TenSyGrid Project to improve the computational performance of these models.

Bibliography

[1] PowerWorld Corporation. *Machine Model GENQEC Equations*. Tech. rep. Accessed: December 19, 2025. PowerWorld Corporation, 2023. URL: https://www.powerworld.com/files/GENQEC-Equations.pdf.

[2] Christoph Kaufmann, Georg Pangalos, and Gerwald Lichtenberg. "Implicit multilinear modeling of limiters in power systems". In: *at - Automatisierungstechnik* 70.2 (2022), pp. 156–166. DOI: 10.1515/auto-2021-0133.

[3] Leandro Samaniego et al. "An Approach to Multi-Energy Network Modeling by Multilinear Models". In: *2024 European Control Conference (ECC)*. IEEE. 2024, pp. 1522–1527. DOI: 10.23919/ECC64448.2024.10591039.

[4] eRoots Analytics S.L. *VeraGrid: Open-Source Power System Modelling and Simulation Platform*. https://veragrid.org. Version 7.0+. Open-source under the MIT license. 2024.

[5] *PES TR1: Dynamic Models for Steam and Hydro Turbines in Power System Studies*. Tech. rep. IEEE Committee Report, Power System Engineering Committee, Accessed: 10 November 2025. New York, USA: IEEE Power Engineering Society, 1992. URL: https://site.ieee.org/fw-pes/files/2013/01/PES_TR1.pdf.

[6] *IEEE Standard 421.5-2016: Recommended Practice for Excitation System Models for Power System Stability Studies*. Tech. rep. Accessed: 10 November 2025. New York, USA, 2016. DOI: 10.1109/IEEESTD.2016.7553421. URL: https://home.engineering.iastate.edu/~jdm/ee554/IEEEstd421.5-2016RecPracExSysModsPwrSysStabStudies.pdf.

[7] Vinícius Albernaz Lacerda et al. "Phasor and EMT models of grid-following and grid-forming converters for short-circuit simulations". In: *Electric Power Systems Research* 223.109662 (Oct. 2023). DOI: 10.1016/j.epsr.2023.109662.

[8] CoLib Project. *CoLib Model Library*. https://colib.net/models/index.html. Accessed: 7 November 2025. 2025.

[9] Christoph Kaufmann et al. *Small-Signal Stability Analysis of Power Systems by Implicit Multilinear Models*. 2025. DOI: 10.48550/arXiv.2510.16534. arXiv: 2510.16534 [eess.SY].